DEUTERIUM NMR STUDY OF LIQUID CRYSTALS

MOWEI CHENG

A Thesis

Submitted to the Faculty of Graduate Studies

in Partial Fulfillment of the Requirements

for the Degree of

MASTER OF SCIENCE

Department of Physics

University of Manitoba

Winnipeg, Manitoba

THE UNIVERSITY OF MANITOBA

FACULTY OF GRADUATE STUDIES

*****

COPYRIGHT PERMISSION PAGE

Deuterium NMR Study of Liquid Crystals

BY

Mowei Cheng

A Thesis/Practicum submitted to the Faculty of Graduate Studies of The University of Manitoba in partial fulfillment of the requirements of the degree

of

Master of Science

Abstract

Deuterium nuclear magnetic resonance (NMR) spectroscopy was used to explore molecular motions in the mesophases of S-4-(2-methylbutyloxy)carbonylphenyl1 4-(10-undecenyloxy)-benzoate(MBPUB-d_2), and a mixture of 4-n-octyloxy-4'-cyanobiphenyl (8OCB-d_{17}) and 4-n-hexyloxy-4'-cyanobiphenyl (6OCB). The deuteron quadrupolar and Zeeman spin-lattice relaxation times were measured as a function of temperature in the nematic, smectic A and reentrant nematic phases of the mixture and in the smectic A phase of MBPUB at two different Larmor frequencies.

For MBPUB, the quadrupolar and proton-deuteron dipole splittings of the ring were also measured. The derived spectral densities of motion at different temperatures were analyzed simultaneously using a small-step rotational diffusion model. Internal ring rotations were superimposed onto the overall motion. For this particular chiral molecule, we found an anomalous behaviour $(D_\perp > D_\parallel)$ which is different from non-chiral rodlike liquid crystals.

For the 8OCB/6OCB mixture, the additive potential method is employed to model the quadrupolar splittings, from which the potential of mean torque is parametrized, and the order parameter tensor for an "average" conformer is determined. A decoupled model is used to describe correlated internal motions of the end chain, which are independent

of the molecular reorientation. The latter motion is treated using the small-step rotational diffusion model, while the former motion is described using a master rate equation. In addition, the order director fluctuations were also taken into account in order to fit experimental results in the nematic phase.

Acknowledgments

I wish to express thanks to my supervisor, Professor R. Y. Dong, for his guidance and support throughout my years as a graduate student. He spent lots of time in helping me in the laboratory, answering my questions, proof reading this thesis as well as solving problems that are related to me being an international student. From him, I gained a great deal of knowledge of NMR, liquid crystals and how to conduct research independently.

A special thank goes to Mr. Norm Finlay for his great help in fixing experimental apparatus and solving many practical problems. I also thank Professor G. C. Tabisz, Mr. J. Zhao and Mr. C. Morcombe for their kind assistance.

A special thank extends to my parents X. R. Cheng and W. Y. Zou, my aunt X. Z. Cheng, my uncle C. Xiao and my wife H. Y. Niu for all their understanding and support over the years. Finally, I would like to thank Ms. B. Monita for her helps in using the Scientific Word software.

Table of Contents

List of Figures

List of Abbreviations

6OCB 4-n-hexyloxy-4'-cyanobiphenyl

8OCB-d_{17} 4-n-octyloxy-4'-cyanobiphenyl

AP additive potential

DMR Deuterium Nuclear Magnetic Resonance

EFG electric field gradient

FID Free Induction Decay

J-B Jeener-Broekaert

MBPUB-d_2 S-4-(2-methylbutyloxy)carbonylphenyl1 4-(10-undecenyloxy)-benzoate

NMR Nuclear Magnetic Resonance

ODF Order Director Fluctuations

RIS rotational isomeric state

TZ Tarroni-Zannoni

1 Introduction

Liquid crystals are composed of flexible organic molecules and are capable of forming different ordered structures in their mesophases. Nuclear Magnetic Resonance (NMR), is a non-invasive tool that is specific to various nuclei, and through perturbation by interactions between a nucleus and its surroundings, NMR is sensitive to molecular structure, orientation, configuration and dynamics [1.1].

Rowell and co-workers [1.2] were the first to demonstrate that deuterium is an excellent spin probe for studying liquid crystals. The deuteron NMR spectra are often characterized by well resolved quadrupolar doublets that may contain some fine structures due to dipole-dipole interactions [1.3], and the thermally driven molecular motion can be studied by spin relaxation time measurements.

1.1 Liquid Crystal

It is known [1.4] that some organic molecules may pass through an intermediate phase known as mesophase or liquid crystal phase when changing from a solid to a liquid. The molecules forming the liquid crystal mesophase are called mesogens. The molecule in a solid crystal lattice are stationary, keeping a fixed location and orientation in space. In a liquid, molecules are free enough to move to any location and orientation. In liquid crystals, the long molecular axes tend to line up along one direction, (called the director

$\hat{n}$), like a solid, but also have a certain amount of disorder, like a liquid. This means that molecules are not in a completely frozen state, but are able to exhibit restricted motions. It is this anisotropic motion which makes liquid crystals so interesting from both a scientific and an industrial standpoint.

Liquid crystals may be divided into two categories: thermotropic and lyotropic. Transitions to the intermediate states may be brought about by purely thermal processes (thermotropic mesomorphism) or by the influence of solvents (lyotropic mesomorphism). There are several different phases in thermotropic crystals. The structure nature of mesophases is influenced by the molecular shape and therefore depends on whether the liquid crystal is formed by rod-like or disk-like molecules.

The nematic liquid crystal phase is characterized by molecules that have no positional order but tend to point in the same direction (along the director $\hat{n}$). Thus it differs from the isotropic liquid in that molecules are spontaneously oriented with their molecular long axes approximately parallel. The physical properties of the system vary with the average alignment of molecules with the director $\hat{n}$. For almost all the thermotropic nematics known so far, the nematic phase is uniaxial, which means that there exists rotational symmetry around the director $\hat{n}$.

A special class of nematic liquid crystals is called chiral nematic. Chiral refers to the unique ability to selectively reflect one component of circularly polarized light. The

term chiral nematic is used interchangeably with cholesteric. Here molecules tend to align somewhat twisted with respect to one another. This causes the director to rotate in space in a helical fashion. The distance for a 360° rotation of the director is called the pitch [1.5].

The smectic state is another distinct mesophase of liquid crystal substances. Molecules in this phase show a degree of translational order not present in the nematic. In the smectic state, the molecules maintain the general orientational order of nematics, but also tend to align themselves in layers or planes. Motion is restricted to within these planes, and separate planes are observed to flow past each other. The increased order means that the smectic state is more "solid-like" than the nematic. Therefore, smectic phase normally occurs at temperatures below the nematic phase, except in reentrant phenomena.

In the smectic-A mesophase, the director is perpendicular to the smectic plane, and there is no particular positional order in the layer. For the smectic-B mesophase, orientation of the director is still perpendicular to the smectic plane, but the molecules are arranged into a network of hexagons within the layer. In the smectic-C mesophase, molecules are arranged as in the smectic-A mesophase, but the director is at a constant tilt angle with respect to the normal of smectic plane.

As in the nematic, the smectic-C mesophase has a chiral state designated C*. Consistent with the smectic-C, the director makes a tilt angle with respect to the smectic layer.

The difference is that this tilt angle rotates around the planar normal from layer to layer forming a helix.

In some smectic mesophases, the molecules are weakly coupled to the various layers above and below them. Therefore, a small amount of three dimensional order is observed. Smectic-G is an example demonstrating this type of arrangement.

There is also a special nematic phase called the reentrant nematic phase. Some samples, when cooling down from the isotropic phase, possess two or more nematic phases, with one or more smectic phase(s) in between. The reentrant nematic phase refers to the lower temperature phase below a more ordered phase like smectic-A. The 8OCB/6OCB mixture sample, for the composition approximately 28 wt % of 6OCB, exhibits a reentrant nematic phase at atmospheric temperature [1.8], i.e., one observes a transition from the smectic-A phase to a nematic phase on either heating or cooling the system. The collective packing of the chains, which enhances the stability of the S_A phase, is frustrated in a reentrant phase.

1.2 Basic NMR

Nuclear Magnetic Resonance (NMR) is an analytical method in which the effect of magnetic fields on nuclear spins [1.6] is observed. In particular, nuclear spins of different orientations in an applied magnetic field have different energies. These energies corre-

spond to radio frequencies and when the nuclear spins are exposed to radio waves of certain frequencies, transitions between energy levels may occur. NMR may be used to provide information regarding such things as the structure of molecules or molecular interactions.

Nuclear magnetic resonance is observed in systems which contain magnetic moments as well as angular momenta. Assemblies of nuclei contain both of these properties. Consider a nucleus of spin I. It has a magnetic moment μ and angular momentum L. Since these two vectors are colinear, the following equation may be written:

$$\mu = \gamma L \tag{1.1}$$

where γ, a scalar quantity, is called the gyromagnetic ratio and is dependent on the size and the state of the nucleus. Quantum theory leads to the expression:

$$L = \hbar I \tag{1.2}$$

The application of a magnetic field H_0 produces an interaction energy of

$$H_Z = -\vec{\mu} \cdot \vec{H}_0 = -\gamma \hbar \vec{I} \cdot \vec{H}_0 \tag{1.3}$$

where the $\vec{H}_0$ is taken along the Z_L direction of a laboratory frame. The effect of an alternating magnetic field is analyzed by modeling it as two rotating components, each of

amplitude H_1 and one rotating clockwise while the other counterclockwise.

$$\begin{aligned} \vec{H}_R &= H_1 (\hat{\imath} \cos\omega t + \hat{\jmath} \sin\omega t) \\ \vec{H}_L &= H_1 (\hat{\imath} \cos\omega t - \hat{\jmath} \sin\omega t) \end{aligned} \tag{1.4}$$

The $\vec{H}_R$ and $\vec{H}_L$ differ just by ω changing sign to $-\omega$. Without loss in generality, we use $\omega = \omega_z \hat{k}$ to write

$$\vec{H}_1(t) = H_1 (\hat{\imath} \cos\omega_z t + \hat{\jmath} \sin\omega_z t) \tag{1.5}$$

The motion of the magnetic moment in a magnetic field satisfies the following equation:

$$\frac{d\vec{\mu}}{dt} = \gamma \frac{d\vec{L}}{dt} = \gamma \vec{\mu} \times \vec{H} \tag{1.6}$$

The total macroscopic magnetization, $\vec{M}$, is the vector sum of the magnetic moments. Thus, the vector sum of equation (1.6) produces the equation of motion

$$\frac{d\vec{M}}{dt} = \gamma \vec{M} \times \vec{H} = \vec{M} \times \gamma \left[\vec{H}_0 + \vec{H}_1 (t) \right] \tag{1.7}$$

The analysis is simplified if the time dependence of H_1 is eliminated. This is accomplished by a conversion of the above equation to a coordinate system that rotates about the Z_L axis at the frequency ω_z. This rotating coordinate system will be used unless otherwise stated. In this system, H_1 is static, and since the axis of rotation is in the same direction as H_0, H_0 is static. If H_1 is assumed to be along the x axis of the rotating frame, the

equation (1.7) becomes

$$\frac{d\vec{M}}{dt} = \vec{M} \times \left[\hat{k}\left(\omega_z + \gamma H_0\right) + \hat{\imath}\gamma H_1\right] \tag{1.8}$$

By definition, resonance is the condition which occurs when the alternating field effectively cancels the effect of the static field. Therefore, as the condition of resonance is approached, $\omega_z + \gamma H_0$ approaches zero. This may be emphasized by rewriting equation (1.8) using $\omega_z = -\omega$.

$$\begin{aligned} \frac{d\vec{M}}{dt} &= \vec{M} \times \gamma \left[\hat{k}\left(H_0 - \frac{\omega}{\gamma}\right) + \hat{\imath}H_1\right] = \vec{M} \times \gamma \vec{H}_{eff} \\ \vec{H}_{eff} &= \hat{k}\left(H_0 - \frac{\omega}{\gamma}\right) + \hat{\imath}H_1 \end{aligned} \tag{1.9}$$

Equation (1.9) states that in the rotating frame, the magnetization acts as though it is effectively experiencing a static magnetic field $\vec{H}_{eff}$.

When the resonance condition($\omega = \gamma H_0$) is satisfied, $\vec{H}_{eff} = \vec{H}_1$. Then, only H_1 is left to interact with the magnetization, M, of the system of nuclear spins. If H_1 is arbitrarily assigned to the x axis of the rotating frame, then M will experience a torque due to the magnetic field H_1 and thus, will rotate, or precess, about the x axis of the rotating frame. That is, it will always precess perpendicular to H_1 , with a frequency γH_1 . The angle through which M rotates in a period of time t_p is given by:

$$\theta = \gamma H_1 t_p \tag{1.10}$$

A 90° pulse is to rotate M from the direction along H_0 to the y axis in the rotating frame. This expression is fundamental to pulse methods of NMR.

From equation (1.10), it would seem that once M is rotated to an angle θ, M will stay in this new position indefinitely. In reality, however, the spins of the nuclei interact with their surroundings which cause a decay of M back to its original state. This process is a first-order relaxation process and is characterized by a time called the spin-lattice relaxation time, T_1. The nuclear spins will also come to equilibrium with each other. The time required for this to occur is called the spin-spin relaxation time T_2. After perturbation of the system, M_z will eventually decay back to its equilibrium value of M_0, M_x and M_y will eventually decay back to their equilibrium value of zero. The evolution of M_z towards M_0 modifies the energy of the spin system through exchange of energy with the lattice, whereas the decrease in transverse magnetization components does not produce such an exchange of energy and is the effect of spin-spin interactions among nuclear spins. The lattice is defined as the degrees of freedom other than the spin system in the molecular system of interest. Motions that contribute to T_1 also contribute to T_2 so that $T_2 \leqslant T_1$ is always satisfied.

The two relaxation times were defined as a result of the determination by F. Bloch in terms of three differential equations to describe the motion of macroscopic magnetization in the presence of an applied magnetic field. Bloch started from equation (1.7) and to

account for relaxation discussed above, he obtained three phenomenological equations, called the Bloch equations [1.7],

$$\begin{aligned}
\frac{dM_z}{dt} &= \gamma\left(\vec{M}\times\vec{H}\right)_z - \frac{M_z - M_0}{T_1} \\
\frac{dM_x}{dt} &= \gamma\left(\vec{M}\times\vec{H}\right)_x - \frac{M_x}{T_2} \\
\frac{dM_y}{dt} &= \gamma\left(\vec{M}\times\vec{H}\right)_y - \frac{M_y}{T_2}
\end{aligned} \tag{1.11}$$

The Bloch equations may be solved for each situation with its appropriate boundary conditions. It should be noted that T_1 and T_2 are often called the longitudinal and transverse relaxation times respectively, because they describe the decay of M along and perpendicular to the static field.

1.3 Thesis Outline

Chapter 1 gives the introduction to liquid crystals and basic NMR concepts. The basic NMR theory is presented in Chapter 2. Chapters 3 and 4 give the theories of the molecular dynamics of liquid crystal necessary for the current study including the Tarroni-Zannoni (TZ) Model, director fluctuations and decoupled model of internal and overall motions for flexible chain dynamics. The experimental methods are given in Chapter 5. Chapters 6 and 7 present the experimental results and discussion of studied liquid crystal samples.

References

[1.1] Paul Ukleja and Daniele Finotello, "NMR Review"

[1.2] J. C. Rowell, W. D. Philips, L. R. Melby, and M. Panar, J. Chem. Phys., **43**, 3442, 1965

[1.3] R. Y. Dong, "Liquid Crystalline Samples: Deuterium NMR"

[1.4] Case Western Reserve University, "Polymers & Liquid Crystals", 1998 (http://plc.cwru.edu)

[1.5] R. Y. Dong, "Nuclear Magnetic Resonance of Liquid Crystals", Spinger-Verlag, N.Y., 1997

[1.6] L. Friesen, Undergraduate Thesis, Brandon University, 1992

[1.7] T. C. Farrar, E. D. Becker, "Pulse and Fourier Transform NMR", Academic Press, New York and London, 1971

[1.8] P. E. Cladis, Phys. Rev. Lett., **35**, 48, 1975

2 Basic ^{2}H NMR Theory

2.1 Nuclear Electric Quadrupole Interaction

So far we have considered only the magnetic interaction of the nucleus with the surroundings. We know that the effect of the nuclear charge is to determine the electron orbits and where the nucleus sits in a molecule. However, we have not considered any electrical effects on the energy required to reorient the nucleus in a magnetic field. There is, therefore, an electrostatic energy that varies with the nuclear orientation [2.1].

The quadrupole Hamiltonian H_Q arises from an electrostatic interaction of the nuclear quadrupole moment ($Q_{\alpha\beta}$) with the external electric field gradient (efg), $V_{\alpha\beta}(= \nabla\vec{E})$ at the position of nucleus. $V_{\alpha\beta}$ and $Q_{\alpha\beta}$ are defined as

$$\begin{aligned} Q_{\alpha\beta} &= e \sum_{k(protons)} (3x_{\alpha k}x_{\beta k} - \delta_{\alpha\beta}r_k^2) \\ V_{\alpha\beta} &= \left(\frac{\partial^2 V}{\partial x_\alpha \partial x_\beta}\right)_{nuclei} \end{aligned} \tag{2.1}$$

where $x_{\alpha k}$ ($\alpha = 1, 2, 3$) stands for x, y, or z, respectively for the kth proton, $r_k^2 = x_{1k}^2 + x_{2k}^2 + x_{3k}^2$, and V is the potential due to sources external to nucleus. Thus, a quadrupole Hamiltonian H_Q is given by

$$H_Q = \frac{1}{6}\sum_{\alpha,\beta} V_{\alpha\beta}Q_{\alpha\beta} \tag{2.2}$$

Using Clebsch-Gordon coefficients and the Wigner-Eckart theorem, equation (2.2) can be rewritten as

$$H_Q = \frac{eQ}{6I(2I-1)} \sum_{\alpha,\beta} V_{\alpha\beta} \left[\frac{3}{2} \left(I_\alpha I_\beta + I_\beta I_\alpha \right) - \delta_{\alpha\beta} I^2 \right] \tag{2.3}$$

where

$$eQ = \langle II\eta \mid e \sum_{k(protons)} (3x_{3k}^2 - r_k^2) \mid II\eta \rangle$$

The effective quadrupole interaction of Eq. (2.3) applies for an arbitrary orientation of the rectangular coordinates $\alpha = x, y, z$. The tensor coupling to the symmetric (in x, y, z) tensor $V_{\alpha\beta}$ can be simplified by choosing a set of principal axes in which $V_{\alpha\beta} = 0$ for $\alpha \neq \beta$. In terms of these axes, along with Laplace's equation $\sum_\alpha V_{\alpha\alpha} = 0$, we have

$$H_Q = \frac{eQ}{4I(2I-1)} \left[V_{zz} \left(3I_z^2 - I^2 \right) + \left(V_{xx} - V_{yy} \right) \left(I_x^2 - I_y^2 \right) \right] \tag{2.4}$$

Equation (2.4) shows that only two parameters are needed to characterize the derivatives of the potential; V_{zz} and $V_{xx} - V_{yy}$. It is customary to define two symbols, η and q, called the asymmetry parameter and the field gradient, by the equations

$$\begin{aligned} eq &= V_{zz} \\ \eta &= \frac{V_{xx} - V_{yy}}{V_{zz}} \end{aligned} \tag{2.5}$$

Generally, the efg asymmetry parameter is small for deuterons, ($\eta \leqslant 0.05$) and can be neglected.

Usually the elements of $V_{\alpha\beta}$ are known in a molecular-fixed coordinate system but the spin operators I_x, I_y and I_z are quantized in the laboratory frame defined by the external magnetic field. Therefore, it is necessary to rotate efg tensor through coordinate transformation using Euler Angles (α, β, γ) (Fig. 2.1).

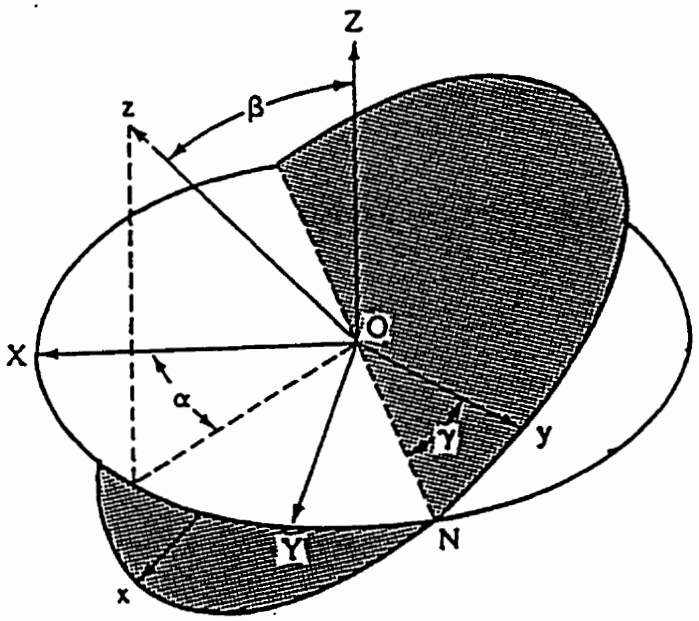

Figure 2.1 Rotations used in the definition of Euler Angles

Accordingly $V_{\alpha\beta}$ should be expressed by its irreducible tensor components V_m^2 $(m = 0, \pm 1, \pm 2)$.

$$\begin{aligned} V_0^2 &= \sqrt{\frac{3}{2}} V_{zz} \\ V_{\pm 1}^2 &= V_{zx} \pm i V_{zy} = 0 \quad \text{(in PAS)} \\ V_{\pm 2}^2 &= \frac{1}{2}(V_{xx} - V_{yy}) \pm i V_{xy} = \frac{1}{2}\eta V_{zz} \quad \text{(in PAS)} \end{aligned} \tag{2.6}$$

The transformation from one frame to another simply involves the Wigner rotation matrices $D^2_{mm'}(\alpha, \beta, \gamma)$ [2.2].

$$V^2_{m'} = \sum_{m=-2}^{2} D^2_{mm'}(\alpha, \beta, \gamma) V^2_m \tag{2.7}$$

2.2 Nuclear Dipole-Dipole Interaction

The dipole Hamiltonian H_D arises from direct dipole-dipole interactions between the nuclear magnetic moments and has the form [2.3]

$$H_D = \frac{\mu_0}{4\pi} \frac{\gamma_i \gamma_j \hbar^2}{r_{ij}^3} \vec{I}_i \cdot \hat{D}_{ij} \cdot \vec{I}_i \tag{2.8}$$

where μ_0 is the magnetic vacuum permeability, r_{ij} is the internuclear distance, and $\hat{D}_{ij}$, the dipole coupling tensor, may be defined by $(\delta_{ij} - 3e_i e_j)$ with e_i $(i = x, y, z)$ being x, y, and z components of a unit vector pointing from one spin to the other. The internuclear vector $\vec{r}_{ij}$ has orientation $\left(\theta_{ij}, \phi_{ij}\right)$ in the laboratory frame $\left(\vec{B}_0 \parallel Z\right)$. The dipolar Hamiltonian

can be written in terms of irreducible spherical tensor operators [2.4],

$$H_D = -\frac{\mu_0}{4\pi}\frac{\gamma_i\gamma_j\hbar^2}{r_{ij}^3}\sum_{m=-2}^{2}(-1)^m F_{2,-m}\left(\theta_{ij},\phi_{ij}\right)T_{2,m} \tag{2.9}$$

The functions $F_{2,m}$ describe the orientation and $T_{2,m}$ contain the spin operators

$$\begin{aligned}
T_{2,0} &= \frac{1}{\sqrt{6}}\left(3I_{iz}I_{jz} - \vec{I}_i\cdot\vec{I}_j\right)\\
T_{2,\pm1} &= \mp\frac{1}{2}\left(I_{iz}I_j^{\pm} + I_i^{\pm}I_{jz}\right)\\
T_{2,\pm2} &= \frac{1}{2}I_i^{\pm}I_j^{\pm}\\
F_{2,0}\left(\theta,\phi\right) &= \sqrt{\frac{3}{2}}\left(3\cos^2\theta - 1\right)\\
F_{2,\pm1}\left(\theta,\phi\right) &= \mp 3\sin\theta\cos\theta\exp\left(\pm i\phi\right)\\
F_{2,\pm2}\left(\theta,\phi\right) &= \frac{3}{2}\sin^2\theta\exp\left(\pm 2i\phi\right)
\end{aligned} \tag{2.10}$$

where $I^{\pm} = I_x \pm iI_y$. In the high-field approximation, H_D may be treated as a first-order perturbation on H_Z and only the part ($m = 0$) of the spin interaction that commutes with I_z is retained, i.e., neglect the nonsecular terms ($m \neq 0$) and retain the term with $m = 0$ to give a truncated dipole Hamiltonian,

$$H_D = -\frac{\mu_0}{4\pi}\frac{\gamma_i\gamma_j\hbar^2}{r_{ij}^3}P_2\left(\cos\theta_{ij}\right)\left[3I_{iz}I_{jz} - \vec{I}_i\cdot\vec{I}_j\right] \tag{2.11}$$

where the Legendre polynomial $P_2\left(x\right) = \left(3x^2 - 1\right)/2$. The truncated dipole Hamiltonian may also be used at low field if axial symmetry about the Z axis exists for the molecular system.

The indirect, electron-mediated interaction has the same form as the direct dipole interaction

$$H_J = \hbar \vec{I}_i \cdot \hat{J}_{ij} \cdot \vec{I}_j \tag{2.12}$$

with the indirect spin-spin coupling tensor $\hat{J}_{ij}$. An important difference is that the $\hat{D}_{ij}$ has no scalar part while $\hat{J}_{ij}$ does. In comparison with the direct dipole interactions, H_J is normally small in liquid crystals and will be ignored hereon.

2.3 Motionally Averaged Hamiltonian

In mesophases, molecules do not rotate isotropically as in normal liquid. Therefore spin Hamiltonians may not be averaged out by rotations. The averaging of Hamiltonian under rotations may be easily studied when it can be expressed in terms of irreducible tensor operator, $T^{\lambda}_{L,m}$ and $R^{\lambda}_{L,m}$ [2.3].

$$H_\lambda = C_\lambda \sum_L \sum_{m=-L}^{L} (-1)^m R^{\lambda}_{L,-m} T^{\lambda}_{L,m} \tag{2.13}$$

where λ indicates the coupling mechanism (e.g. dipolar and quadrupolar) and C_λ is an appropriate coupling constant (e.g., $C_\lambda = eQ/2I(2I-1)$ for quadrupolar interaction). For the quadrupolar interaction, $R^{\lambda}_{L,m}$ are non-zero only when $L = 2$ and will be replaced by V^2_m. In the PAS system, the components with $m = \pm 1$ vanish.

In the laboratory frame, the spin parts are constant while the spatial parts V_m^2 are time-averaged under rotations to give $\langle V_m^2 \rangle$. Now the Euler angle $\Omega = (\alpha', \beta', \gamma')$ are necessary to bring the laboratory system into principle axis system. The time-averaged quadrupolar Hamiltonian is

$$\overline{H_Q} = \frac{eQ}{2I(2I-1)} \sum_{mm'} (-1)^m \langle D^{2*}_{-m,m'}(\alpha', \beta', \gamma') \rangle V^2_{m'} T_{2,m} \tag{2.14}$$

Note that here the inverse rotation transformation matrix $D^{L*}_{-m,m'}$ is used and the $T_{2,m}$ are given by

$$\begin{aligned} T_{2,0} &= \frac{1}{\sqrt{6}} \left(3I_z^2 - I^2\right) \\ T_{2,\pm 2} &= \frac{1}{2} \left(I^{\pm}\right)^2 \end{aligned} \tag{2.15}$$

For a deuteron ($I = 1$) spin with axially symmetric electric field gradient ($\eta = 0$), the time-averaged quadrupole Hamiltonian is given by

$$\overline{H_Q} = \frac{eQ}{2I(2I-1)} \langle V_0^2 \rangle T_{2,0} \tag{2.16}$$

In liquid crystals, molecules are aligned by their neighbors through the potential of mean torque. The preferred direction of the molecular alignment in a uniaxial phase is called the director $\hat{n}$. Suppose the director is parallel to the external field. The transformation should be carried out through an intermediate molecular frame (x_M, y_M, z_M)

$$\langle V_0^2 \rangle = \sum_m \overline{D^{2*}_{0,m}(\phi, \theta, \psi)} D^{2*}_{m,0}(\alpha, \beta, \gamma) V_0^2 \tag{2.17}$$

where (α, β, γ) are the Euler angles that carry the molecular frame to PAS frame, while (ϕ, θ, ψ) are the Euler angles that transform the laboratory frame into the molecular frame. Note that $D^{2*}_{m,0}(\alpha, \beta, \gamma) = D^{2*}_{m,0}(\alpha, \beta)$ since the value of γ is irrelevant when $m' = 0$. The time-averaged quadrupolar Hamiltonian is from Eqs. (2.16) and (2.17):

$$\overline{H_Q} = \hbar\omega_Q \left[I_z^2 - I(I+1)/3\right] \tag{2.18}$$

where

$$\omega_Q = \frac{3}{4}\frac{e^2qQ}{\hbar}\sum_m \overline{D^2_{0,m}(\theta, \psi)} D^2_{m,0}(\alpha, \beta)$$

The time-averaged Wigner rotation matrices $\overline{D^2_{0,m}(\theta, \psi)}$ are the order parameters in a uniaxial phase and can be written in the form of a Cartesian order tensor $\hat{S}$ which is a symmetric and traceless 3×3 matrix. Thus $\hat{S}$ has a maximum of five independent nonzero components, defined by [2.5]

$$\begin{aligned}
S_{zz} &= \overline{D^2_{0,0}} \\
S_{xx} - S_{yy} &= \sqrt{\frac{3}{2}}\left(\overline{D^2_{0,2}} + \overline{D^2_{0,-2}}\right) \\
S_{xy} &= i\sqrt{\frac{3}{8}}\left(\overline{D^2_{0,-2}} - \overline{D^2_{0,2}}\right) \\
S_{xz} &= \sqrt{\frac{3}{8}}\left(\overline{D^2_{0,-1}} - \overline{D^2_{0,1}}\right) \\
S_{yz} &= i\sqrt{\frac{3}{8}}\left(\overline{D^2_{0,-1}} - \overline{D^2_{0,1}}\right)
\end{aligned} \tag{2.19}$$

The ordering of molecules in a mesophase may be described by a singlet probability

function $P(\theta,\psi)$. The molecular frame may be chosen such that $P(\theta,\psi)$ is an even function of the polar angles. This results in $\overline{D^2_{0,\pm1}} = 0$ and $\overline{D^2_{0,2}} = \overline{D^2_{0,-2}}$. When $\overline{H_Q}$ is non-zero, the Zeeman line is now split into two lines with a quadrupolar splitting (Fig. 2.2)

$$\delta\nu_Q = \frac{3}{2}\frac{e^2qQ}{\hbar}\left[S_{zz}\left(\frac{3}{2}\cos^2\beta - \frac{1}{2}\right) + \frac{1}{2}\left(S_{xx} - S_{yy}\right)\sin^2\beta\cos 2\alpha\right] \qquad (2.20)$$

where (α,β) are polar angles of $C-D$ vector in the molecular frame.

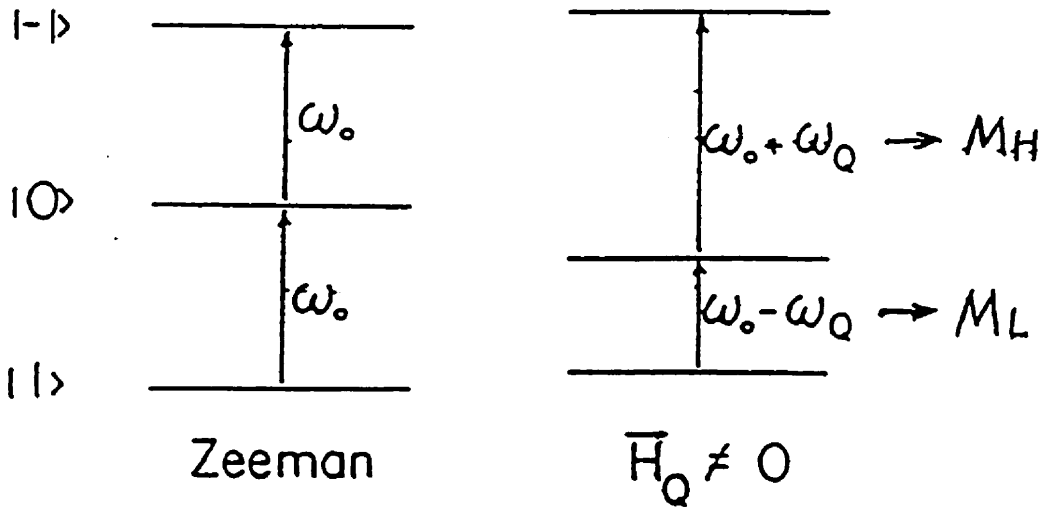

Figure 2.2 Energy levels diagram of a deuteron ($\eta = 0$) in a large external magnetic field.

Similarly, the time-averaged dipole Hamiltonian is given by

$$\begin{aligned} \overline{H_D} &= -\Delta_D \left[I_{iz} I_{jz} - \frac{1}{4} \left(I_i^+ I_j^- + I_i^- I_j^+ \right) \right] \\ \Delta_D &= \frac{\mu_0 \gamma^2 \hbar^2}{2\pi r_{ij}^3} \sum_m \overline{D_{0,m}^{2*}(\theta, \psi)} D_{m,0}^{2*}(\alpha_{ij}, \beta_{ij}) \end{aligned} \tag{2.21}$$

The dipole splitting is then given by

$$\delta\nu_D = \frac{3\mu_0}{8\pi^2} \frac{\gamma^2 \hbar}{r_{ij}^3} \left[S_{zz} \left(\frac{3}{2} \cos^2 \beta_{ij} - \frac{1}{2} \right) + \frac{1}{2} \left(S_{xx} - S_{yy} \right) \sin^2 \beta_{ij} \cos 2\alpha_{ij} \right] \tag{2.22}$$

where $(\alpha_{ij}, \beta_{ij})$ are polar angles of internuclear vector $\vec{r}_{ij}$ in the laboratory frame. For molecules of cylindrical symmetry, the molecular biaxial parameter $(S_{xx} - S_{yy})$ is identical to zero.

2.4 Order Parameters

The orientation of rigid molecules in a mesophase can be specified by a singlet distribution function $f(\Omega)$, where Ω denotes the Euler angles (ϕ, θ, ψ) that transform between the molecular and director frames. The average of any single-molecule property $X(\Omega)$ over the orientation of all molecules is defined by

$$\langle X \rangle = \int_0^{2\pi} d\phi \int_0^{\pi} d\theta \sin\theta \int_0^{2\pi} d\psi X(\Omega) f(\Omega) \tag{2.23}$$

In terms of the Wigner rotation matrices of rank L, the orientation distribution func-

tion can be expanded as

$$f(\Omega) = \sum_{L=0}^{\infty} \sum_{m,m'=-L}^{L} \frac{2L+1}{8\pi^2} \alpha_{Lm'm} D_{m'm}(\Omega) \tag{2.24}$$

Applying the normalization condition, the expanded coefficients $\alpha_{Lm'm}$ can be obtained, i.e. $\alpha_{Lm'm} = \langle D_{m'm}(\Omega) \rangle$. For rodlike molecules, the pseudo-potential $V(\Omega)$ is independent of ϕ and ψ due to the uniaxial phase symmetry and the cylindrical molecular symmetry, respectively. The orientation distribution function becomes

$$\begin{aligned} f(\Omega) &= \frac{f(\theta)}{4\pi^2} \\ f(\theta) &= \sum_{L=0}^{\infty} \frac{2L+1}{2} \langle P_L(\cos\theta) \rangle P_L(\cos\theta) \end{aligned} \tag{2.25}$$

where $P_L(\cos\theta) = D_{00}^{L}(\theta)$. The expansion coefficients in $f(\theta)$ are the orientational order parameter $\langle P_L \rangle$ given by

$$\langle P_L \rangle = \int_0^1 P_L(\cos\theta) f(\cos\theta) d(\cos\theta) \tag{2.26}$$

Among all the orientation parameters of different ranks, only second rank order parameters can be determined from the line position in NMR spectra.

2.5 Molecular Field Theory of Flexible Molecules: The AP Method

The constituent molecules of liquid crystals usually contain an aromatic core and one or more flexible side chains. NMR studies of order parameter profiles in these molecules have

revealed that the ordering of their rigid segments varies with respect to each other and with temperature [2.3]. Since the flexible chains not only occupy space but also contribute to the anisotropic potential and interactions, they are partially responsible for the molecular ordering in liquid crystals. In attempting to interpret the deuterium quadrupolar splittings $\Delta\nu_i$, which are both temperature dependent and site dependent, it is necessary to assume that molecular conformation is independent of molecular orientation, thereby separating the internal and overall motions.

The additive potential (AP) method was first introduced by Marcelja [2.10] explicitly to take the alkyl chain into account in calculating physical properties of liquid crystals, and was subsequently extended by Emsley, Luckhurst and Stockley [2.11] . Due to internal degree of freedom, the chain therefore does not always exist in an all-trans conformation. An additional average is needed for flexible molecules because different conformational states are available to the molecules. In doing so, it is necessary to determine all of the allowed conformations and their relative weights $p_{eq}(n)$, the equilibrium probability for finding a molecule in the *nth* conformation. This can be handled by using the rotational isomeric state (RIS) model [2.12] which allows each of the methylene groups to be either in the *trans* (t) state or in one of the two possible *gauche* ($g^{\pm}$) states. Though there are many internal modes, we shall restrict to rotations about the $O-C$ and $C-C$ bonds in an alkyloxy chain. The $g^{\pm}$ states are obtained by $\pm 112^{\circ}$ rotations about the $C-C$

bond. In this model, only states in the potential minima are assumed to be appreciably populated. This is due to the very steep potential barriers between these minima. The *gauche* states have higher internal energy in comparison to that of the *trans* state by an amount of E_{tg}. When the chain contains a g^+g^- or a g^-g^+ linkage, an additional internal energy $E_{g^\pm g^\mp}$ should be added because these linkages bring parts of the chain near to one another, the so-called "pentane effect". The E_{tg} values for gaseous alkanes lie between 2.1 and 3.2 KJ/mol, while the $E_{g^\pm g^\mp}$ value is about three times larger [2.12].

In modeling the quadrupolar splittings ($\Delta\nu_i$) for the methylene C_i deuterons, one uses

$$\Delta\nu_i = \frac{3}{2} q_{CD}^{(i)} P_2(\cos\Theta)\, S_{CD}^{(i)} \tag{2.27}$$

where $q_{CD}^{(i)} = (e^2qQ/h)_i$, is the quadrupolar coupling constant for C_i deuterons and is taken as 165kHz and 185kHz for methylene and ring deuterons, respectively. Θ is the angle between the director and the external magnetic field. $\Theta = 0$ for the 6OCB and 8OCB liquid crystal samples whose director is aligned along the external magnetic field. $S_{CD}^{(i)}$ is a weighted average of the segmental order parameter. Suppose that $S_{\alpha\beta}^n$ represents an order parameter tensor which describes the orientational order of the nth rigid conformer. Then in the principal axis (X, Y, Z) frame of the nuclear quadrupolar interaction, one has

$$S_{CD}^{(i)} = \sum_n p_{eq}(n) \left[S_{ZZ}^{n,i} + \frac{\eta^{(i)}}{3} \left(S_{XX}^{n,i} - S_{YY}^{n,i} \right) \right] \tag{2.28}$$

where the sum is over all possible configurations in the chain. The C-D bond is taken to

be along the axis Z (i.e., $q_{CD}^{(i)} = q_{ZZ}^{(i)} = V_{ZZ}^{(i)}$). $\eta^{(i)}$, the asymmetry parameter of the electric field gradient, is defined by

$$\eta^{(i)} = \frac{q_{XX}^{(i)} - q_{YY}^{(i)}}{q_{ZZ}^{(i)}} \tag{2.29}$$

For the methylene deuterons, $\eta = 0$ is a very good approximation. To evaluate $p_{eq}(n)$, one needs both the internal energy $U_{int}(n)$ and external potential energy $U_{ext}(n, \omega)$ of the *nth* conformer. The internal energy is assumed to depend on the number of *gauche* linkages (N_g) and the number of $g^{\pm}g^{\mp}$ linkages ($N_{g^{\pm}g^{\mp}}$) in the chain of the *nth* conformer:

$$U_{int}(n) = N_g E_{tg} + N_{g^{\pm}g^{\mp}} E_{g^{\pm}g^{\mp}} \tag{2.30}$$

while the external potential energy also depends on the orientation ω of the director in a molecular frame of the *nth* conformer.

The potential of mean torque $U_{ext}(n, \omega)$ is responsible for the alignment of a conformer and results from the molecular field of its neighbors. It depends on the conformational state n of the molecule and on the polar angles ω of the director in a frame that is attached to a particular rigid segment of the conformer. To minimize the number of parameters, it is assumed that the molecule can be divided into a small number of rigid segments. Each segment is associated with an interaction tensor that is independent of the conformation. The interaction tensor of the molecule is calculated by transforming the interaction tensors from their segmental axis system into a common system and then adding them together.

This is the basis of additive potential (AP) method. The potential of mean torque for particular conformation can be approximated by a second-rank term [2.13]

$$U_{ext}(n,\omega) = -\sum_{m} (-1)^m \epsilon^n_{2,m} C_{2,-m}(\omega) \tag{2.31}$$

where $C_{2,-m}(\omega)$ is a modified spherical harmonic of rank 2. $\epsilon^n_{2,m}$, the interaction tensor for conformation n, is given by

$$\epsilon^n_{2,m} = \sum_{j} \epsilon^j_{2,m}(n) \tag{2.32}$$

where the sum over j is to add together interaction tensors of all rigid subunits. In the jth segmental axis frame, $\epsilon^j_{2,r}$ represents the local interaction of the jth rigid subunit and is assumed to be independent of the conformation. Let $\epsilon^a_{2,r}$ and $\epsilon^c_{2,r}$ represent the interaction tensors of the aromatic core and of each C-C segment, respectively. If both of them are assumed to have cylindrical symmetry, the unique components of $\epsilon^a_{2,r}$ and $\epsilon^c_{2,r}$ are X_a and X_{cc}, respectively. In this simplification, the number of interaction parameters required to calculate $\epsilon^n_{2,m}$ is reduced to two. The segmental interaction tensor $\epsilon^j_{2,m}(n)$ vary with conformation because their components need to be expressed in a common molecular frame. This dependence is expressed in

$$\epsilon^j_{2,m}(n) = \sum_{r} D^{2*}_{m,r}\left(\omega^n_j\right) \epsilon^j_{2,r} \tag{2.33}$$

where $D^{2*}_{m,r}\left(\omega^n_j\right)$ is the second-rank Wigner rotation matrix, and ω^n_j denotes the set of Euler angles needed to transform between axes in the jth segment and the common

molecular frame. The $p_{eq}(n)$ is given by

$$p_{eq}(n) = \exp\left[-U_{int}(n)/k_BT\right] Q_n/Z \tag{2.34}$$

where Q_n, the orientation partition function of conformation n, is

$$Q_n = \int \exp\left[-U_{ext}(n,\omega)/k_BT\right] d\omega \tag{2.35}$$

and Z, the conformation-orientational partition function, is

$$Z = \sum_n \exp\left[-U_{int}(n)/k_BT\right] Q_n \tag{2.36}$$

Now the order parameter for a particular direction k in the conformation n may be evaluated in the principal (x,y,z) frame of $U_{ext}(n,\omega)$ according to

$$S_{kk}^{n,i} = \sum_{\alpha}^{x,y,z} S_{\alpha\alpha}^{n} \cos^2\theta_{\alpha k}^{n,i} \tag{2.37}$$

where $\theta_{\alpha k}^{n,i}$ denotes angles for the $C_i - ^2 H$ bond between the $k(=X,Y,Z)$ axis and a principal axis $\alpha(=x,y,z)$. $S_{\alpha\alpha}^{n}$, the principal components of the Saupe ordering matrix for the conformer n, may be written as

$$\begin{aligned} S_{xx}^{n} &= \frac{1}{2}\left(\sqrt{6}\left\langle d_{0,2}^2 \cos 2\psi\right\rangle_n - \left\langle d_{0,0}^2\right\rangle_n\right) \\ S_{yy}^{n} &= -\frac{1}{2}\left(\sqrt{6}\left\langle d_{0,2}^2 \cos 2\psi\right\rangle_n + \left\langle d_{0,0}^2\right\rangle_n\right) \\ S_{zz}^{n} &= \left\langle d_{0,0}^2\right\rangle_n \end{aligned} \tag{2.38}$$

In order to evaluate the averages of the reduced rotation matrices, it is advantageous to describe the director orientation in the principal axis system of $U_{ext}(n,\omega)$. Hence, the constructed interaction tensor $U_{ext}(n,\omega)$ is first diagonalized to obtain the interaction tensor components $X^n_{2,0}$ and $X^n_{2,\pm 2}$ for the conformer n. In the principal frame

$$U_{ext}(n,\omega) = -\left[X^n_{2,0} d^2_{0,0}(\theta) + 2X^n_{2,2} d^2_{0,2}(\theta)\cos 2\psi\right] \tag{2.39}$$

Using $a_n = X^n_{2,0}/k_BT$ and $b_n = 2X^n_{2,2}/k_BT$, the order parameters of the nth conformer can be evaluated [2.14]

$$\begin{aligned}
\left\langle d^2_{0,0}\right\rangle_n &= 2\pi \int_0^\pi P_2(\cos\theta)\, I_0\left[b_n d^2_{0,2}(\theta)\right] \exp\left[a_n d^2_{0,0}(\theta)\right] \sin\theta d\theta / Q_n \\
\left\langle d^2_{0,2}\cos 2\psi\right\rangle_n &= 2\pi \int_0^\pi d^2_{0,2}(\theta)\, I_1\left[b_n d^2_{0,2}(\theta)\right] \exp\left[a_n d^2_{0,0}(\theta)\right] \sin\theta d\theta / Q_n
\end{aligned} \tag{2.40}$$

where Q_n becomes

$$Q_n = 2\pi \int_0^\pi I_0\left[b_n d^2_{0,2}(\theta)\right] \exp\left[a_n d^2_{0,0}(\theta)\right] \sin\theta d\theta \tag{2.41}$$

and $I_n(x)$, the nth order modified Bessel function is given by

$$I_n(x) = \frac{1}{\pi}\int_0^\pi \cos n\varphi \exp(x\cos\varphi)\, d\varphi \tag{2.42}$$

2.6 Spectral Densities

In the quadrupolar Hamiltonian, there are fluctuating terms because of the rotation and/or collective motions of liquid-crystal molecules. The autocorrelation function $G_{m_L}(t)$

may be defined in terms of the Wigner rotation matrix $D^2_{m_L m_M}(\Omega_{LM})$ in the fluctuation Hamiltonian

$$G_{m_L}(t) = \sum_{m_M} \left[d^2_{m_M 0}(\theta)\right]^2 \langle \left[D^2_{m_L m_M}(\Omega_{LM}(0)) - \overline{D^2_{m_L m_M}}\right] \times \left[D^{2*}_{m_L m_M}(\Omega_{LM}(t)) - \overline{D^{2*}_{m_L m_M}}\right] \rangle \quad (2.43)$$

Now $\Omega_{LM} (\equiv \alpha, \beta, \gamma)$ denotes the Euler angles that transform between a molecular frame attached to the molecular core and the laboratory frame, θ is the angle between the C-D bond and the z_M axis of the molecular frame, and m_L and m_M are the projection indices for a tensor of rank two in the laboratory and molecular z axis, respectively. The autocorrelation functions for molecular reorientation (terms with angle brackets in Eq. (2.27)) are generally given by a sum of decreasing exponentials [2.6], and,

$$G^2_{m_L m_M}(t) = C_{m_L m_M} \sum_{j=1}^{3} a^{(j)}_{m_L m_M} \exp\left[-t/\tau^{(j)}_{m_L m_M}\right] \quad (2.44)$$

where $C_{mn} = \left(\langle |D_{m,n}|^2 \rangle - \overline{\left(D^2_{0,0}\right)^2}\right)$, is the mean square of the Wigner rotation matrices. The correlation times $\tau^{(j)}_{m_L m_M}$ depend on the order parameter $\langle P_2 \rangle$ and on the variation of the rotational diffusion tensor components with temperature. The $a^{(j)}_{m_L m_M}$ represent normalized weights of each exponential whose time constant

$$\tau^{(j)}_{m_L m_M} = \frac{b^{(j)}_{m_L m_M}}{6D_\perp + b^{(j)}_{m_L m_M} m_M \left(D_\parallel - D_\perp\right)} \quad (2.45)$$

where $D_\parallel$ refers to motion about the molecular z_m axis, while $D_\perp$ refers to motion of the z_M axis. The coefficients $a^{(j)}_{m_L m_M}$, $b^{(j)}_{m_L m_M}$ and $C_{m_L m_M}$ for all the correlation functions are

given numerically as polynomials in $\langle P_2 \rangle$ and their expansion coefficients are tabulated in Table I of Ref. [2.7] for a Maier-Saupe potential. Equations (2.28) and (2.29) are expressed in the notation of Dong [2.8].

From the standard spin relaxation theory [2.9] for deuterons ($I = 1$), the Zeeman $\left(T_{1Z}^{-1}\right)$ and quadrupolar $\left(T_{1Q}^{-1}\right)$ spin-lattice relaxation rates are given in terms of spectral densities $J_{m_L}(m_L\omega_0)$ by

$$\begin{aligned} T_{1Z}^{-1} &= J_1(\omega_0) + 4J_2(2\omega_0) \\ T_{1Q}^{-1} &= 3J_1(\omega_0) \end{aligned} \tag{2.46}$$

The spectral density is simply the Fourier transform of the autocorrelation function $G_{m_L}(t)$

$$\begin{aligned} J_{m_L}(m_L\omega) &= \frac{3\pi^2}{2}(q_{CD})^2 \int_0^\infty G_{m_L}(t)\cos(m_L\omega t)\,dt \\ &= \frac{3\pi^2}{2}(q_{CD})^2 \sum_{m_M}\left[d^2_{m_M}(\theta)\right]^2 C_{m_L m_M} \\ &\quad \times \sum_j a^{(j)}_{m_L m_M} \frac{\left(\tau^{(j)}_{m_L m_M}\right)^{-1}}{\left[(m_L\omega)^2 + \left(\tau^{(j)}_{m_L m_M}\right)^{-2}\right]} \end{aligned} \tag{2.47}$$

where $q_{CD} = e^2qQ/h$ ($\eta = 0$ is assumed) is the nuclear quadrupolar coupling constant.

2.7 Summary

In this chapter, we have introduced quadrupolar and dipolar splittings, and showed how they are related to the order parameters. The AP method is outlined and will be used to understand segmental order parameters for a flexible chain. The spectral densities of motion are also described.

References

[2.1] C. P. Slichter, "Principles of Magnetic Resonance", Third Edition. 1990

[2.2] J. J. Sakurai, "Modern Quantum Mechanics". Addison-Wesley Publishing Company, Inc., 1985

[2.3] R. Y. Dong, "Nuclear Magnetic Resonance of Liquid Crystals", Spinger-Verlag, N.Y., 1997

[2.4] A. Abragam, "The principle of Nuclear Magnetism", Clarendon, Oxford, 1961

[2.5] C. Zannoni, "The Molecular Physics of Liquid Crystals", edited by G. R. Luckhurst and G. W. Gray, Academic, New York, 1979

[2.6] P. L. Nordio and P. Busolin, J. Chem. Phys., **55**, 5485, 1971; P. L. Nordio, G. Rigatti and U. Segre, J. Chem. Phys., **56**, 2117, 1972; Mol. Phys., **25**, 129, 1973

[2.7] R. R. Vold and R. L. Vold, J. Chem. Phys., **88**, 1443, 1988

[2.8] R. Y. Dong, Molecular Physics, **88**, 4979, 1996

[2.9] J. P. Jacobsen, H. K. Bildsoe, and K. Schumburg, J. Magn. Reson. **23**, 153, 1976; S. B. Ahmad, K. J. Packer and J. M. Ramsden. Mol. Phys. **33**, 857, 1977; R. R. Vold and R. L. Vold, J. Chem. Phys., **66**, 4018, 1977

[2.10] S. Marcelja, J. Chem. Phys., **60**, 3599, 1974

[2.11] J. W. Emsley, G. R. Luckhurst and C. P. Stockley, Proc. R. Soc. London A, **381**, 117, 1982

[2.12] P. J. Flory, "Statistical Mechanics of Chain Molecules". Inter Science, New York, 1969

[2.13] M. A. Cotter, "The molecular Physics in Liquid Crystals", edited by G. R. Luckhurst and G. W. Gray, Academic Press, London, 1979

[2.14] G. R. Luckhurst, C. Zannoni, P. L. Nordio and A. Segre, Mol. Phys., **30**, 1345, 1975

3 Relaxation by Molecular Reorientation and Director Fluctuations

3.1 Introduction

The rotation diffusion model has been widely used to describe molecular reorientation since Debye's introduction [3.1]. It can be used to interpret nuclear relaxation in isotropic liquids [3.2]. More recently, it has been used extensively as a model to account for the nuclear spin relaxation behavior in thermotropic liquid crystals. Each molecule is characterized by a rotational diffusion tensor $\overline{D}$, normally defined in a frame fixed on the molecule. The principal components of $\overline{D}$ are D_{xx}, D_{yy} and D_{zz}. For a symmetric rotor reorienting in a uniaxial potential with rotational diffusion constants $D_{xx} = D_{yy} \neq D_{zz}$, solutions were first presented by Nordio and co-workers [3.3, 3.4]. The Nordio model was used in numerous experimental studies including NMR. There were some attempts to analyze the deuterium spin relaxation behavior of non-cylindrically symmetric molecules, e.g., several asymmetric planar rotors, as rotational diffusions of a symmetric top in a uniaxial potential [3.5, 3.6], but worries persisted that the less than perfect fits were caused by using this approximation. The rigorous treatment of the asymmetric rotor has been published by Tarroni and Zannoni [3.7] (TZ model), and the solutions use terms up to rank 40 in the Wigner basis set. There is a recent report in which the TZ model was

applied to study the deuteron relaxation of a biaxial solute Fluorene-d_{10} in the Licrystal phase 5 [3.8].

3.2 Correlation Functions

The rotational diffusion model assumes a stochastic Markov process [3.2, 3.3, 3.9] for molecular reorientation in which each molecule moves in time as a sequence of small angle steps caused by collisions with its neighboring molecules and under the influence of an anisotropic potential set up by its neighbors. The orientational correlation function can be written as

$$G^{LL'}_{mn,m'n'}(t) = \int\int d\Omega_0 d\Omega P(\Omega_0) D^{L*}_{mn}(\Omega_0) \times P(\Omega_0 \mid \Omega t) D^{L'}_{m'n'}(\Omega) \tag{3.1}$$

where for simplicity, we use m and n to represent the m_L, the projection index in the laboratory frame and m_M, the projection index in the molecular frame, respectively. $\Omega \equiv (\alpha, \beta, \gamma)$ denotes Euler angles, $P(\Omega_0 \mid \Omega t)$ is the conditional probability of finding a molecule at orientation Ω at time t if the orientation of the molecule was Ω_0 at $t = 0$, and the equilibrium probability, $P(\Omega)$ is given by the Boltzmann distribution:

$$P(\Omega) = \frac{\exp[-U(\Omega)/kT]}{\int d\Omega \exp[-U(\Omega)/kT]} \tag{3.2}$$

where k is the Boltzmann constant and T is the temperature. $U(\Omega)$ is the potential of mean torque acting on the molecule [3.10], and its symmetry is determined by the sym-

metry of the molecule and that of the mesophase. In the long time limit, the orientational correlation function may be non-zero in an anisotropic medium, and is given by

$$G^{LL'}_{mn,m'n'}(\infty) = \langle D^{L}_{0m}(\Omega_0)\rangle \langle D^{L'}_{0m'}(\Omega)\rangle \delta_{m0}\delta_{m'0} \tag{3.3}$$

This long time plateau has to be subtracted from $G^{LL'}_{mn,m'n'}(t)$ to ensure its decay to zero in equilibrium.

For cylindrical molecules in the uniaxial phase, the potential of mean torque is governed by the β angle only, i.e. $U(\Omega) = U(\beta)$. For asymmetric molecules reorienting in a uniaxial phase, the potential of mean torque depends on two Euler angles, i.e. $U(\Omega) = U(\beta, \gamma)$ [3.11]. Now the effective anisotropic potential $U(\Omega)$ can be expressed in terms of Wigner matrices as

$$\frac{U(\beta,\gamma)}{kT} = \sum_{Jq} a_{Jq} D^{J}_{0q}(\beta,\gamma) \tag{3.4}$$

and the orientational order parameters, averages of the Wigner rotation matrices $D^{L}_{mn}(\Omega)$, are

$$\langle D^{L}_{0m}\rangle = \int d\Omega P(\beta,\gamma)\, D^{J}_{0m}(\beta,\gamma) \tag{3.5}$$

If the molecular reorientation takes place through a sequence of small angular steps, the evolution of the conditional probability $P(\Omega_0|\Omega t)$ can be described [3.7, 3.12] by a

differential equations for the rotational diffusion process as

$$\frac{\partial P\left(\Omega_0|\Omega t\right)}{\partial t} = -\sum_{\alpha\beta} L_\alpha D_{\alpha\beta}\left[L_\beta + L_\beta\left(\frac{U\left(\Omega\right)}{kT}\right)\right] P\left(\Omega_0|\Omega t\right) \tag{3.6}$$

where L_β ($= L_x$, L_y or L_z) is a component of a dimensionless angular momentum operator $\vec{L}$, and $\overline{D}$ is a rotational diffusion tensor. Here we choose a molecule-fixed frame in which $\overline{D}$ is diagonal

$$\overline{D} = \begin{pmatrix} D_{xx} & 0 & 0 \\ 0 & D_{yy} & 0 \\ 0 & 0 & D_{zz} \end{pmatrix} = \rho \begin{pmatrix} 1+\epsilon & 0 & 0 \\ 0 & 1-\epsilon & 0 \\ 0 & 0 & \eta \end{pmatrix} \tag{3.7}$$

where

$$\rho = \frac{D_{xx} + D_{yy}}{2}, \epsilon = \frac{D_{xx} - D_{yy}}{D_{xx} + D_{yy}}, \eta = \frac{2D_{zz}}{D_{xx} + D_{yy}} \tag{3.8}$$

ϵ is an asymmetry parameter of the diffusion tensor, going from -1 to $+1$, η is the ratio between diffusion around z_M axis (spinning motion) and diffusion of the z_M axis itself(tumbling motion) which is expressed by ρ. In the cylindrical symmetry limit (ρ becomes $D_\perp$, η becomes $D_\parallel/D_\perp$ and ϵ reduces to 0), the diffusion matrix is reduced to the Nordio limit.

Now, back to the more general case with non-zero ϵ, equation (3.6) becomes

$$\begin{aligned}\frac{1}{\rho}\frac{\partial P(\Omega_0|\Omega t)}{\partial t} &= -(1+\epsilon)\left[L_x^2 + L_x\left(L_x\frac{U(\Omega)}{kT}\right)\right]P(\Omega_0|\Omega t) \\ &\quad -(1+\epsilon)\left[L_y^2 + L_y\left(L_y\frac{U(\Omega)}{kT}\right)\right]P(\Omega_0|\Omega t) \\ &\quad -\eta\left[L_z^2 + L_z\left(L_z\frac{U(\Omega)}{kT}\right)\right]P(\Omega_0|\Omega t) \\ &= \vec{\Gamma}P(\Omega_0|\Omega t) \end{aligned} \tag{3.9}$$

where $\vec{\Gamma}$ is the diffusion operator which, for the purpose of numerical calculations, can be rewritten using a unitary transformation as

$$\begin{aligned}\hat{\Gamma} &= P^{-1/2}(\Omega)\,\vec{\Gamma}\,P^{1/2}(\Omega) \\ &= -\left[\nabla^2 + \frac{1}{2}\left(\nabla^2\frac{U(\Omega)}{kT}\right) - \frac{1}{4}\left(L_+\frac{U(\Omega)}{kT}\right)\left(L_-\frac{U(\Omega)}{kT}\right) - \frac{1}{4}\eta\left(L_z\frac{U(\Omega)}{kT}\right)^2\right] \\ &\quad -\epsilon\{\frac{1}{2}\left(L_+^2 + L_-^2\right) + \frac{1}{4}\left[\left(L_+^2 + L_-^2\right)\frac{U(\Omega)}{kT}\right] \\ &\quad -\frac{1}{8}\left[\left(L_+\frac{U(\Omega)}{kT}\right)^2 + \left(L_-\frac{U(\Omega)}{kT}\right)^2\right]\} \end{aligned} \tag{3.10}$$

where $P(\Omega)$ is the equilibrium distribution, and

$$\nabla^2 = L_x^2 + L_y^2 + \eta L_z^2 \tag{3.11}$$

and

$$L_\pm = L_x \pm iL_y \tag{3.12}$$

is the angular momentum step operator. When $\epsilon = 0$, the above operator $\hat{\Gamma}$ is the same as that used by Nordio and his co-workers. The diffusion equation in this symmetrized form is given by

$$\frac{1}{\rho}\frac{\partial \hat{P}\left(\Omega_0|\Omega t\right)}{\partial t} = \hat{\Gamma}\hat{P}\left(\Omega_0|\Omega t\right) \tag{3.13}$$

where

$$\hat{P}\left(\Omega_0|\Omega t\right) = P^{-1/2}\left(\Omega\right) P\left(\Omega_0|\Omega t\right) P^{1/2}\left(\Omega_0\right) \tag{3.14}$$

is the symmetrized conditional probability. The symmetrized diffusion equation can be given a convenient matrix representation in a basis of normalized Wigner matrices:

$$\mathcal{D}^{L}_{mn}\left(\Omega\right) = \sqrt{\frac{2L+1}{8\pi^2}} D^{L}_{mn}\left(\Omega\right) \tag{3.15}$$

by expanding the symmetrized conditional probability $\hat{P}\left(\Omega_0|\Omega t\right)$,

$$\hat{P}\left(\Omega_0|\Omega t\right) = \sum_{Lmn} C_{Lmn}\left(\Omega_0, t\right) \mathcal{D}^{L}_{mn}\left(\Omega\right) \tag{3.16}$$

The expanding coefficients $C_{Lmn}\left(\Omega_0, t\right)$ at time zero can be evaluated using the initial condition $\hat{P}\left(\Omega_0|\Omega t\right) = \delta\left(\Omega - \Omega_0\right)$. Thus,

$$C_{Lmn}\left(\Omega_0, 0\right) = \mathcal{D}^{L*}_{mn}\left(\Omega_0\right) \tag{3.17}$$

Substituting Eq. (3.16) in Eq. (3.13), multiplying both sides on the left for $\mathcal{D}^{L*}_{mn}\left(\Omega\right)$ and integrating over Ω we obtain the system of linear differential equations

$$\frac{1}{\rho}\dot{C}\left(t\right) = \hat{R}C\left(t\right) \tag{3.18}$$

where

$$\left(\hat{R}^m\right)_{L'n'Ln} = \int d\Omega \mathcal{D}^{L'*}_{mn'}(\Omega)\,\hat{\Gamma}\mathcal{D}^{L}_{mn}(\Omega) \tag{3.19}$$

The explicit expression of the matrix elements $R_{L'm'n',Lmn}$ depend on the orienting potential $U(\Omega)$ and can be obtained from Appendix A for the important specific case of a mean-field potential containing only second rank interactions. In solving the above linear diffusion equations, a unitary eigenvector matrix $\hat{X}^m$ which diagonalizes the self-adjoint diffusion matrix $\hat{R}^m$ should be introduced

$$\hat{R}^m\hat{X}^m = \hat{X}^m\hat{r}^m \tag{3.20}$$

where $\hat{r}^m$ is a diagonal matrix that contains the eigenvalues of $\hat{R}^m$. The formal solution is

$$C^m(t) = \hat{X}^m \exp\left(t\rho\hat{r}^m\right)\left(\hat{X}^m\right)^T C^m(0) \tag{3.21}$$

Considering the matrix elements of $\hat{X}^m$ and substituting the zero time coefficients, we obtain

$$C_{Jmp}(\Omega_0,t) = \sum_K\sum_{J'p'}\left(\hat{X}^m\right)_{Jp,K}\exp\left(t\rho\hat{r}^m\right)\left(\hat{X}^m\right)^T_{J'p',K}\mathcal{D}^{J'*}_{mp'}(\Omega_0) \tag{3.22}$$

where we have used single index K to label the eigenvalues of the diffusion matrix, $\hat{R}^m$. Using the un-normalized Wigner matrices, the symmetrized conditional probability can

be written as

$$\begin{aligned}\hat{P}\left(\Omega_0|\Omega t\right) &= \frac{1}{8\pi^2}\sum_{Kq}\sum_{Jp}\sum_{J'p'}\sqrt{2J+1}\sqrt{2J'+1}\left(\hat{X}^q\right)_{Jp,K} \\ &\quad\times\exp\left(t\rho\hat{r}_K^q\right)\left(\hat{X}^q\right)_{J'p',K} D_{qp}^{J}\left(\Omega\right) D_{qp'}^{J'*}\left(\Omega_0\right) \qquad (3.23)\end{aligned}$$

For $t\rightarrow\infty$ all the exponentials decay to zero except the one corresponding to the eigenvalue $\hat{r}_0^0$. The long time behavior of the symmetrized conditional probability is obtained by

$$\begin{aligned}\lim_{t\rightarrow\infty}\hat{P}\left(\Omega_0|\Omega t\right) &= P^{1/2}\left(\Omega_0\right)P^{1/2}\left(\Omega\right) \\ &= \frac{1}{8\pi^2}\sum_{J''p'}\sum_{J'''p'''}\sqrt{2J''+1}\sqrt{2J'''+1} \\ &\quad\times\left(\hat{X}^0\right)_{J''p'',0}\left(\hat{X}^0\right)_{J'''p''',0} D_{0p''}^{J''}\left(\Omega\right) D_{0p'''}^{J'''}\left(\Omega_0\right) \qquad (3.24)\end{aligned}$$

Eq. (3.1) can be rewritten as

$$\begin{aligned}G_{mnn'}^{LL'}\left(t\right) &= \int d\Omega_0 P^{1/2}\left(\Omega_0\right) D_{mn}^{L*}\left(\Omega_0\right) \\ &\quad\times\int d\Omega P^{1/2}\left(\Omega\right)\times P\left(\Omega_0|\Omega t\right) D_{m'n'}^{L'}\left(\Omega\right) \qquad (3.25)\end{aligned}$$

Substituting Eq. (3.23) and Eq. (3.24) in Eq. (3.25), the correlation functions can be

expressed as

$$
\begin{aligned}
G_{mnn'}^{LL'}(t) &= \sum_{K} \exp\left(t\rho\hat{r}_{K}^{n}\right) \sum_{Jp} \sum_{J'p'} \sum_{J''J'''} \frac{\sqrt{(2J+1)(2J'+1)(2J''+1)(2J'''+1)}}{(2L+1)(2L'+1)} \\
&\quad \times \left(\hat{X}^{m}\right)_{Jp,K} \left(\hat{X}^{m}\right)_{J'p',K} \left(\hat{X}^{0}\right)_{J''n'-p;0} \left(\hat{X}^{0}\right)_{J'''n-p';0} C\left(J''', J', L; 0, m\right) \\
&\quad \times C\left(J''', J', L; n-p', p'\right) C\left(J'', J, L'; 0, m\right) C\left(J'', J, L'; n'-p, p\right) \\
&= \sum_{K} \left(b_{mnn'}^{LL'}\right)_{K} \exp\left[t\left(a_{mnn'}^{LL'}\right)_{K}\right] \qquad (3.26)
\end{aligned}
$$

where $C(A, B, C; d, e)$ is the Clebsch-Gordon coefficient, $\left(a_{mnn'}^{LL'}\right)_{K}/\rho$, the decay constants, are the eigenvalues of the Γ matrix, and $\left(b_{mnn'}^{LL'}\right)_{K}$, the relative weights of the exponentials, are the corresponding eigenvectors. In the limit that $G_{mnn'}^{LL'}(t)$ can be reexpressed by a single exponential, then

$$
b_{mnn'}^{LL'} = G_{mnn'}^{LL'}(0) - G_{mnn'}^{LL'}(\infty) \qquad (3.27)
$$

For $L = L' = 2$ and $n = n'$, b_{mn}^{22} reduces to the $\kappa(m, n)$, the mean square of the Wigner rotation matrices, given by Freed [3.13]. This secion provides the spin relaxation theory to describe the overall reorientation of molecules in uniaxial mesophases.

3.3 Spectral Densities

The spectral densities $J^{(AB)}_{LL'nn'}(m\omega)$ are given by the following sum of Fourier transformation of the correlation functions in Eq. (3.26)

$$J^{(AB)}_{LL'nn'}(m\omega) = \sum_{nn'} A^{Ln*}_{MOL} B^{L'n'}_{MOL} \int_0^\infty G^{LL'}_{mnn'}(t) \exp(-im\omega t)\, dt \tag{3.28}$$

For deuteron NMR experiments, $L = L' = 2$, $A^{Ln*}_{MOL} = \sqrt{3/2}\pi q_{CD} d^2_{n0}(\theta)$, $B^{L'n'}_{MOL} = \sqrt{3/2}\pi q_{CD} d^2_{n'0}(\theta)$ where θ is the angle between the molecular z_M axis and the principal z axis of the efg tensor (e.g., the $C-D$ bond). The spectral densities for a biaxial molecule in uniaxial phases are given by

$$J_m(m\omega) = \frac{3\pi^2}{2}(q_{CD})^2 \sum_{nn'} d^2_{n0}(\theta)\, d^2_{n'0}(\theta) \sum_K \frac{(b^{22}_{mnn'})_K (a^{22}_{mnn'})_K}{(a^{22}_{mnn'})^2_K + (m\omega)^2} \tag{3.29}$$

3.4 The Ring Rotation and Internal Motions

Eq. (3.29) is for deuterons without internal degree of freedom. When the aromatic ring is rotating freely about its para axis with a diffusion constant D_R, the spectral densities are given by [3.7]

$$\begin{aligned} J^{(R)}_m(m\omega) &= \frac{3\pi^2}{2}\left(q^{(R)}_{CD}\right)^2 \sum_{nn'}\sum_p \left[d^2_{p0}(\theta_{R,Q})\right]^2 d^2_{n,p}(\theta_{M,R})\, d^2_{n',p}(\theta_{M,R}) \\ &\quad \times \sum_K \frac{(b^{22}_{mnn'})_K \left[(a^{22}_{mnn'})_K + (1-\delta_{p0}) D_R\right]}{\left[(a^{22}_{mnn'})_K + (1-\delta_{p0}) D_R\right]^2 + (m\omega)^2} \end{aligned} \tag{3.30}$$

where the strong collision limit is used for ring rotations, $\theta_{R,Q}$ is the angle between the $C-D$ bond and the para axis, and $\theta_{M,R}$, the angle between the para axis and the molecular z_M axis, usually can be set to zero. Now the following more general spectral densities are obtained for the case with internal motions

$$J_m^{(i)}(m\omega) = \frac{3\pi^2}{2}\left(q_{CD}^{(i)}\right)^2 \sum_{nn'}\sum_{K}\sum_{l=0}^{\infty} \frac{(b_{mnn'}^{22})_K \left[(a_{mnn'}^{22})_K + C_{nn'l}\right]}{\left[(a_{mnn'}^{22})_K + C_{nn'l}\right]^2 + (m\omega)^2}\Gamma(n,n',l) \qquad (3.31)$$

where $C_{nn'l}$ is related to the correlation time of internal motion and $\Gamma(n,n',l)$ is a function describing the internal motions. The ring internal motion could be free rotation, restricted motion, or π flip of ring around its para-axis, etc. For the special case that the ring is fixed on the molecular frame, i.e., the internal motion is frozen, only one term inside $\sum_l$ survives ($\Gamma(n,n',l) = \delta_{l0}$ and $C_{nn'l} = 0$) and Eq. (3.31) goes back to Eq. (3.29). For deuterons residing in flexible chains, the spectral density for the chain internal motions (described by a rate equation) has a form similar to Eq. (3.31) except the internal function $\Gamma(n,n',l)$ now includes the chain geometric information and eigenvectors of the rate matrix, and the $C_{nn'l}$ is related to the eigenvalues of jump rate matrix. The explicit expression will be given in Chapter 4.

3.5 Director Fluctuations

There are several motional processes(e.g., reorientation, director fluctuations) that take place simultaneously and may cause spin relaxation in liquid crystals. Because of thermal

fluctuations of the director, the orientation of the director has both spatial and temporal variation. Since there is no long range order of positions among the molecules in nematics, a local (instantaneous) director $\hat{n}(\vec{r})$ may be introduced to represent the average direction of molecules within a neighborhood of any point in the sample. The time interval between molecular collisions is about $10^{-10} \sim 10^{-12}s$. Changes in molecular orientation due to collisions could change the local director on the NMR timescale. Thus, an additional coordinate system is needed to specify the local director $\hat{n}(\vec{r})$. The average director $\hat{n}_0$ is obtained by spatially averaging the local directors over the sample.

The angle $\Omega_{LM}(t)$ in the autocorrelation function (Eq. (2.27)) denotes the orientation of the principal molecular axis (x_M, y_M, z_M) in the laboratory frame (X_L, Y_L, Z_L) frame. The coordinate transformation from the (x_M, y_M, z_M) to the (X_L, Y_L, Z_L) frame must be carried out through successive transformations (Figure 3.1) to account for the fast motions of a molecule and slow collective fluctuations of the director. That is, $\Omega_{LM} \equiv (\Omega', \Omega'')$, where the Euler angle Ω' transform from the molecular frame (x_M, y_M, z_M) to the instantaneous director (x, y, z) frame, Ω'' is used to transform the (x, y, z) frame to the laboratory frame (X_L, Y_L, Z_L). Here we assume the average director $\hat{n}_0$ is parallel to the external field $\vec{B}$, which is used to define the laboratory frame.

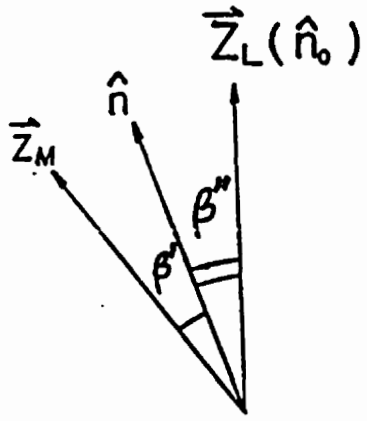

Figure 3.1 A schematic illustration of director fluctuations

In the nematic phase and perhaps "disordered" smectic phases, molecules perform long range cooperative motions, which are slow compared to the rapid reorientation motions of individual molecules. The dynamics of these fluctuations depends on the viscosity coefficients and the elastic coefficients of the liquid crystal. In the continuum theory, the elastic constants K_1, K_2 and K_3 are respectively the splay, twist and bend elastic constants [3.14, 3.15]. Freed has included these collective effects in the spin relaxation theory by allowing the orienting potential $U(\Omega)$ to fluctuate slowly in time. It is assumed that the director shows small fluctuations about its mean position, and that the magnitude of ordering does not change. Then there are three types of terms that contribute to spectral densities: molecular orientation, director fluctuation and a cross-term arising from both

of these motions. According to Pincus [3.16], when director fluctuations are assumed to give small angular amplitude, director fluctuations only contribute to $J_1(\omega)$ in first order approximation. Furthermore, if director fluctuations are slow in comparison to the molecular reorientation, the coupling of these two types of motion would produce a very small cross term [3.17, 3.18]. In the "one constant" approximation, i.e., $K_1 = K_2 = K_3 = K$ and one effective viscosity coefficient is used instead of five Leslie coefficients, the contribution to $J_1(\omega)$ from director fluctuations is [3.17]

$$J_{1DF}(\omega) = \frac{3\pi^2}{2}(q_{CD})^2 \langle P_2 \rangle_0^2 A \left[d_{00}^2(\beta_{M,Q})\right]^2 \Im(\omega_c/\omega)\,\omega^{-1/2} \tag{3.32}$$

where the prefactor A is

$$A = \frac{3kT}{4\sqrt{2}\pi K (D_t + K/\eta)^{1/2}} \tag{3.33}$$

where D_t is the averaged translational self-diffusion constant, ω_c is a high-frequency cutoff frequency, and the cutoff function $\Im(\omega_c/\omega)$ is given by [3.19]

$$\Im(x) = \frac{1}{2\pi}\ln\left[\frac{x - \sqrt{2x} + 1}{x + \sqrt{2x} + 1}\right] + \frac{1}{\pi}\left[\tan^{-1}\left(\sqrt{2x} - 1\right) + \tan^{-1}\left(\sqrt{2x} + 1\right)\right] \tag{3.34}$$

$\Im(\omega_c/\omega)$ is unity at low frequency and becomes small for Larmor frequency much larger than ω_c. η and K are the one constant approximation to the viscosities and the elastic constants of the medium, and $\langle P_2 \rangle_0$ is the nematic order parameter of the molecule relative

to the local director and is related to the usual order parameter $\langle P_2 \rangle$ according to [3.20]

$$\langle P_2 \rangle_0 = \frac{\langle P_2 \rangle}{1 - 3\alpha} \tag{3.35}$$

where the parameter $\alpha = kT/\pi K \lambda_c$ is a measure of the magnitude of director fluctuations.

Standard theories [3.14, 3.21, 3.22] of spin relaxation by director fluctuations in nematics are based on the notion that the mean square amplitude $\langle \beta^2 \rangle$ of the director's displacement is small such that terms of this and higher orders can be neglected. When angular excursions of the local director are not small [e.g., low K or large α], second-order and higher terms are needed and their contributions to $J_{2DF}(2\omega)$ and $J_{0DF}(0)$ become nonzero. When second-order contribution are included in $J_{1DF}(\omega)$, Joghems et al. [3.23] found that it has a correction factor $(1 - 4\alpha)$, which reduces to 1 when α is very small. Then Eq. (3.32) becomes

$$J_{1DF}(\omega) = \frac{3\pi^2}{2} (q_{CD})^2 \langle P_2 \rangle_0^2 A \left[d_{00}^2 (\beta_{M,Q}) \right]^2 \frac{(1 - 4\alpha)}{(1 - 3\alpha)^2} \Im (\omega_c/\omega) \omega^{-1/2} \tag{3.36}$$

For C-D bonds located in the flexible chain, the effect of director fluctuations is made smaller as a result of additional averaging within the chain from the conformational changes. It has been recognized [3.24] in earlier deuterium NMR studies that the spin-lattice relaxation rates for the chain deuterons should scale with the square of their quadrupolar splittings if the spin relaxation is caused only by director fluctuations. Indeed the quadrupolar splittings can give the segmental order parameter of C-D bond at

carbon site i, which is defined by

$$S_{CD}^{(i)} = \left\langle \left\langle P_2\left(\cos\Theta^{(i)}\right)\right\rangle \right\rangle \tag{3.37}$$

where $\Theta^{(i)}$ is the angle between the ith C-D bond and the equilibrium director, $\langle\langle\rangle\rangle$ denotes both the conformational average and overall motion average. In uniaxial phases like the nematic and smectic A, the above equation can be expressed as [3.22]

$$\begin{aligned} S_{CD}^{(i)} &= \left\langle \left\langle P_2\left(\cos\beta_{M,Q}^{(i)}\right) P_2\left(\cos\theta\right)\right\rangle \right\rangle \\ &= \overline{d_{00}^2\left(\beta_{M,Q}^{(i)}\right)}\left\langle P_2\right\rangle \end{aligned} \tag{3.38}$$

where $\overline{d_{00}^2\left(\beta_{M,Q}^{(i)}\right)}$ denotes the conformational average over the $\beta_{M,Q}^{(i)}$ angle of the particular C-D bond with respect to the molecular z_M axis, and θ is the angle between the z_M axis and the equilibrium director. The assumption made for the last step in Eq. (3.38) is that the motional modes for the internal chain motions and for the molecular reorientation are decoupled. Thus, we rewrite Eq. (3.36)

$$J_{1DF}^{(i)}(\omega) = \frac{3\pi^2}{2}\left(q_{CD}^{(i)}\right)^2 A\left(S_{CD}^{(i)}\right)^2 \frac{(1-4\alpha)}{(1-3\alpha)^2}\Im\left(\omega_c/\omega\right)\omega^{-1/2} \tag{3.39}$$

For the sample of mixture of 8OCB-d_{17} and 6OCB, we consider a much smaller contribution as well [3.20]

$$J_{2DF}^{(i)}(\omega) = \frac{3\pi^2}{2}\left(q_{CD}^{(i)}\right)^2 A^2\left(S_{CD}^{(i)}\right)^2 \frac{1}{3\pi(1-3\alpha)^2}\ln\left[1+\left(\frac{\omega_c}{2\omega}\right)^2\right] \tag{3.40}$$

where $q_{CD}^{(i)} = 165$ KHz for methylene deuterons. The calculated spectral densities for the C_i are now given by

$$\begin{aligned} J_1^{(i)}(\omega) &= J_{1R}^{(i)}(\omega) + J_{1DF}^{(i)}(\omega) \\ J_2^{(i)}(2\omega) &= J_{2R}^{(i)}(2\omega) + J_{2DF}^{(i)}(2\omega) \end{aligned} \tag{3.41}$$

where the subscript R is used to denote molecular rotation.

References

[3.1] P. Debye, "Polar Molecules", Dover Publications, Inc., New York, 1928

[3.2] W. T. Huntress, Jr., Adv. Magn. Reson., **4**, 1, 1970

[3.3] P. L. Nordio, P. Busolin, J. Chem. Phys., **55**, 5485, 1971

[3.4] P. L. Nordio, G. Rigatti, U. Segre, J. Chem. Phys., **56**, 2117, 1972

[3.5] W. H. Dickerson, R. R. Vold and R. L. Vold, J. Phys. Chem., **87**, 166, 1983

[3.6] P. R. Luyten, R. R. Vold and R. L. Vold, J. Phys. Chem., **89**, 545, 1985

[3.7] P. A. Beckmann, J. W. Emsley, G. R. Luckhurst and D. L. Turner, Mol. Phys., **59**, 97, 1986

[3.8] S. Huo and R. R. Vold, J. Phys. Chem., **99**, 12391, 1995

[3.9] J. H. Freed, J. Chem. Phys., **66**, 4183, 1977

[3.10] G. R. Luckhurst, "The Molecular Physics of Liquid Crystals", edited by G. R. Luckhurst and G. W. Gray, Academic, New York, 1979

[3.11] C. Zannoni, "The Molecular Physics of Liquid Crystals", edited by G. R. Luckhurst and G. W. Gray, Academic, New York, 1979

[3.12] P. L. Nordio and U. Segre, "The Molecular Physics of Liquid Crystals", edited by G. R. Luckhurst and G. W. Gray, Academic, New York, 1979

[3.13] J. H. Freed, J. Chem. Phys., **66**, 4183, 1977

[3.14] R. Y. Dong, "Nuclear Magnetic Resonance of Liquid Crystals", Spinger-Verlag, N.Y., 1997

[3.15] P. G. de Gennes, "The Physics of Liquid Crystals", Oxford University Press, 1974

[3.16] P. Pincus, Solid State Commum. **7**, 415, 1969

[3.17] J. H. Freed, J. Chem. Phys., **16**, 4183, 1977

[3.18] P. Ukleja, J. Pirs and J. W. Doane, Phys. Rev. A, **14**, 414, 1976

[3.19] J. W. Doane, C. E. Tarr and M. A. Nickerson, Phys. Rev. Lett., **33**, 620, 1974

[3.20] R. L. Vold, R. R. Vold and M. J. Warner, J. Chem. Soc. Faraday Trans. 2, **84**, 997, 1988

[3.21] R. L. Vold, R. R. Vold, "The Molecular Dynamics of Liquid Crystals", G. R. Luckhurst, C. A. Veracini, Eds; Kumer Academic, Dordrecht, 1994

[3.22] C. G. Wade, Annu. Rev. Phys. Chem., **28**, 47, 1977

[3.23] E. A. Joghems, G. van der Zwan, J. Phys., II, **6**, 845, 1996

[3.24] R. Y. Dong, J. Lewis, E. Tomchuk and E. Bock, J. Chem. Phys., **69**, 5314, 1978

4 Internal Dynamics of Flexible Mesogens

4.1 Introduction

Liquid crystals contain organic molecules whose structures usually consist of a rigid core with flexible pendant chains. It is known that molecular flexibility is responsible for variations in the physical properties of liquid crystals. The theoretical treatment of dynamic processes of flexible molecules in an anisotropic medium is not an easy task [4.1 – 4.3]. This often requires a certain number of simplifying assumptions which may only be justified by comparison of the model predictions and experiments. In modeling quadrupolar splittings in liquid crystals, the rotational isomeric state (RIS) model [4.4] has been used to generate all configurations in the chain, and anisotropic interactions with the neighboring chains are described by a mean-field potential. When modeling internal rotations about each carbon-carbon bond in the pendant chains, the configuration transitions of the chain may be superimposed onto the rotational diffusion of the whole molecule. This implies that the molecular core is "massive" such that its motion is independent of configuration transitions in the chain. This simplifying assumption gives rise to the so-called decoupled model. The RIS model has been extended [4.1] to the time domain in order to describe spin relaxation in flexible nematogens. It involves a master equation [4.1] which describes transitions among all allowed configurations in the pendant chains. To simplify

numerical computations, the overall motion is described by a single average rotational diffusion tensor.

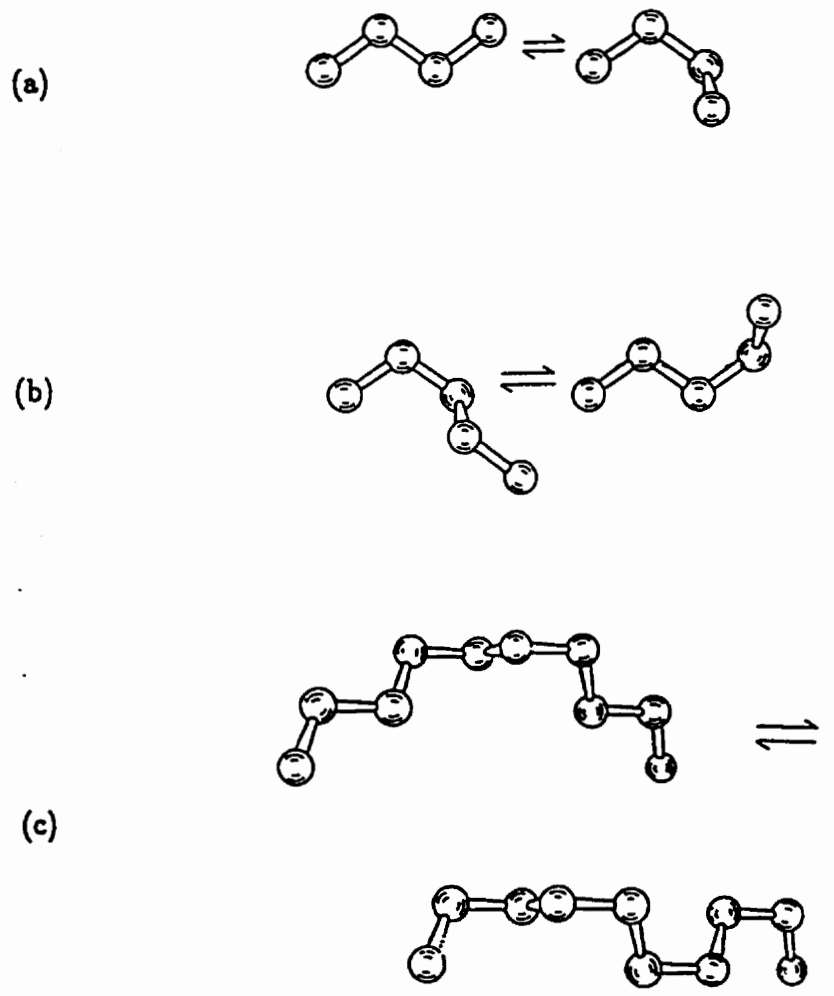

Figure 4.1 The illustration of jump motions of (a) k_1, (b) k_2 and (c) k_3

The decoupled model assumes that in a molecule with N distinct conformations, rotational diffusion tensors for different rotamers do not differ appreciably and that an "average" molecular diffusion tensor may be used to solve the rotation diffusion equation [4.5, 4.6]. Transitions among configurations are described by elementary jump modes [4.7, 4.8] : one-bond(k_1), two-bond(k_2) and three-bond(k_3) motions (Fig. 4.1). A one-bond rotation involves rotation of the last bond in the chain defined as $\{\cdots, l, m, n\} \longrightarrow \{\cdots, l, m, n'\}$, where $\{\}$ denotes the C-C bond orientations in the carbon-carbon backbone of a pendant chain. A two-bond rotation is defined as rotation of the penultimate bond only $\{\cdots, l, m, n\} \longrightarrow \{\cdots, l, m', n'\}$, i.e., it represents motion of the last two C-C bonds in the chain as a pair, with no rotation about the penultimate carbon [4.9]. In the case of a trans bond, i.e., $l = n$, then $n = n'$. A three-bond rotation is a kink motion in the chain, i.e., the interchanging of two alternate bonds, defined as $\{\cdots, i, j, k, \cdots\} \longrightarrow \{\cdots, k, j, i \cdots\}$, is also called the crankshaft transitions.

4.2 Superimposed Rotation Model

In writing the autocorrelation functions that describe both internal and external motions of a flexible mesogen, the Euler angles Ω_{LQ} are used to specify the orientation of the principal axis system of a spin tensor (e.g., efg) with respect to the external magnetic field. Suppose that in a local (α) frame, the orientation ($\Omega_{\alpha Q}$) of a $C_\alpha - {}^2H$ bond is time

independent. A molecule-fixed (M) frame is chosen to coincide with the principal axis system of the rotational diffusion tensor of the molecule. The Euler angles $\Omega_{M\alpha}$ that transform between the local frame and the molecular frame are time dependent due to the internal motions. The angles Ω_{LM} depend on time because of reorientation of the whole molecule. By successive coordinate transformations, the following is obtained:

$$D^2_{m_L 0}\left[\Omega_{LQ}\left(t\right)\right] = \sum_{m_M}\sum_{m_\alpha} D^2_{m_L m_M}\left[\Omega_{LM}\left(t\right)\right] D^2_{m_M m_\alpha}\left[\Omega_{M\alpha}\left(t\right)\right] D^2_{m_\alpha 0}\left(\Omega_{\alpha Q}\right) \tag{4.1}$$

where $\Omega_{\alpha Q}$ is time independent. The autocorrelation function is

$$G_{m_L}\left(t\right) = \left\langle D^2_{m_L 0}\left[\Omega_{LQ}\left(0\right)\right] D^{2*}_{m_L 0}\left[\Omega_{LQ}\left(t\right)\right]\right\rangle - \overline{D^2_{m_L 0}\left[\Omega_{LQ}\left(0\right)\right] D^{2*}_{m_L 0}\left[\Omega_{LQ}\left(t\right)\right]} \tag{4.2}$$

where the second term is to ensure that the autocorrelation functions tend to zero at $t \longrightarrow \infty$ [4.10], Now Eq. (4.2) can be rewritten using Eq. (4.1) as

$$G_{m_L}\left(t\right) = \sum_{m_\alpha}\sum_{m'_\alpha} D^2_{m_\alpha 0}\left(\Omega_{\alpha Q}\right) D^{2*}_{m'_\alpha 0}\left(\Omega_{\alpha Q}\right) G_{m_L m_\alpha m'_\alpha}\left(t\right) \tag{4.3}$$

where

$$\begin{aligned} G_{m_L m_\alpha m'_\alpha}\left(t\right) \;=\; & \sum_{m_M}\sum_{m'_M} \left\langle D^2_{m_L m_M}\left[\Omega_{LM}\left(0\right)\right] D^{2*}_{m_L m'_M}\left[\Omega_{LM}\left(t\right)\right]\right\rangle \\ & \times \left\langle D^2_{m_M m_\alpha}\left[\Omega_{M\alpha}\left(0\right)\right] D^{2*}_{m'_M m'_\alpha}\left[\Omega_{M\alpha}\left(t\right)\right]\right\rangle \\ & - \overline{D^2_{m_L m_M}\left(\Omega_{LM}\right) D^{2*}_{m_L m'_M}\left(\Omega_{LM}\right) D^2_{m_M m_\alpha}\left(\Omega_{M\alpha}\right) D^{2*}_{m'_M m'_\alpha}\left(\Omega_{M\alpha}\right)} \end{aligned} \tag{4.4}$$

because of the usual assumption of decoupling between internal and external motions such that the two motional parts can be averaged separately. When the correlation functions

of internal motions can be written as

$$G_{m_M m'_M m_\alpha m'_\alpha}(t) = \left\langle D^2_{m_M m_\alpha}[\Omega_{M\alpha}(0)]\, D^{2*}_{m'_M m'_\alpha}[\Omega_{M\alpha}(t)] \right\rangle - \overline{D^2_{m_M m_\alpha}(\Omega_{M\alpha})\, D^{2*}_{m'_M m'_\alpha}(\Omega_{M\alpha})} \tag{4.5}$$

then

$$\begin{aligned} G_{m_L m_\alpha m'_\alpha}(t) \;=\; & \sum_{m_M}\sum_{m'_M}[G_{m_L m_M m'_M}(t)\, G_{m_M m'_M m_\alpha m'_\alpha}(t) + G_{m_M m'_M m_\alpha m'_\alpha}(t)\, \overline{D^2_{m_L m_M} D^{2*}_{m_L m'_M}} \\ & + G_{m_L m_M m'_M}(t)\, \overline{D^2_{m_M m_\alpha} D^{2*}_{m'_M m'_\alpha}}] \end{aligned} \tag{4.6}$$

where the correlation functions $G_{m_L m_M m'_M}(t)$ describe the overall motions of molecules, and are given for the TZ model by Eq. (3.26). The complexity here is that the correlation functions are not simply given by a linear combination of products of the correlation functions for each motion. The correlation functions in the above equation include terms that are products of correlation functions for one motion and averaged Wigner matrix components for the other motions. These extra terms are zero for the case of relaxation in normal liquids since the average of Wigner matrix elements are identical to zero. Unlike the random isotropic motions in normal liquids, these terms become nonzero in mesophases because some restricted (preferred) motional degrees of freedom would produce nonzero averages of Wigner matrices. However, Eq. (4.6) may be simplified in certain specific cases. In the superimposed rotation model [4.3], it is assumed that internal rotations about different C-C bonds are independent, and that rodlike molecules

reorienting in uniaxial mesophases with each of their internal motions involve cylindrically symmetric rotation about a single axis, then $m_\alpha = m'_\alpha$ and

$$\begin{aligned} \overline{D^2_{m_L m_M}} &= \delta_{m_L 0}\delta_{m_M 0}\langle P_2\rangle \\ \overline{D^2_{m_M m_\alpha}} &= 0 \end{aligned} \tag{4.7}$$

Therefore, Eq. (4.2) can be written as [4.10]

$$\begin{aligned} G_{m_L}(t) = &\sum_{m_M}\sum_{m'_M}\sum_{m_\alpha}\left[d^2_{m_\alpha 0}(\beta_{\alpha,Q})\right]^2 G_{m_L m_M m'_M}(t)\, G_{m_M m'_M m_\alpha}(t) \\ &+\delta_{m_L 0}\langle P_2\rangle^2 \sum_{m_\alpha}\left[d^2_{m_\alpha 0}(\beta_{\alpha,Q})\right]^2 G_{00m_\alpha}(t) \end{aligned} \tag{4.8}$$

The second term in the above expression represents a cross-term between the internal motions and overall motions, but is zero except when $m_L = 0$, i.e., it is only required in calculating $J_0(0)$, or the spin-spin relaxation times. Otherwise, in calculating $J_1(\omega)$ and $J_2(2\omega)$, or the spin-lattice relaxation times, the overall correlation functions are given by the linear combinations of the products of the correlation functions for each motion. When treating the internal motions further down the chain, additional coordinate frames are needed to carry out successive transformations from a local α frame to the molecular fixed frame.

4.3 Decoupled Model for Correlated Internal Motions

To evaluate the correlation functions in Eq. (4.3), it is necessary to find the conditional probability $P_{il_0}[\Omega_{LM}, t|\Omega_{LM}(0), 0]$ that at time t, the molecule has configuration i and orientation Ω_{LM}, at $t = 0$, the molecule has configuration l and orientation $\Omega_{LM}(0)$. Using the assumption of decoupling internal and external motions, the conditional probability can be expressed as the product of configuration and orientation conditional probabilities:

$$P_{il_0}[\Omega_{LM}, t|\Omega_{LM}(0), 0] = p(i, t|l, 0)\, p[\Omega_{LM}, t|\Omega_{LM}(0), 0] \tag{4.9}$$

Now using the above conditional probability to express the ensemble average in Eq. (4.3),

$$\begin{aligned} G_{m_L}(t) &= \sum_{i,l} \int\int d\Omega_{LM} d\Omega_{LM}(0) \left(D^2_{m_L 0}[\Omega_{LQ}(0)]\, D^{2*}_{m_L 0}[\Omega_{LQ}(t)] - \overline{D^2_{m_L 0} D^{2*}_{m_L 0}} \right) \\ &\quad \cdot \times p_{eq}(l)\, p_{il_0}[\Omega_{LM}, t|\Omega_{LM}(0), 0] \end{aligned} \tag{4.10}$$

where $p_{eq}(l)$ is the probability of occurrence of configuration l at equilibrium. This can be calculated, for example, using the additive potential method. The orientation conditional probability $p[\Omega_{LM}, t|\Omega_{LM}(0), 0]$ was used to evaluate $G^2_{m_L m_M m'_M}(t)$ in chapter 4, and $p(i, t|l, 0) = P_{il_0}(t)$ is required to evaluate internal correlation functions. To evaluate $G_{m_L}(t)$, one needs to transform the electric-field-gradient tensor through successive coordinates to allow for internal motions and reorientation of the molecule. Instead of using many local coordinate systems, it is more convenient to define a coordinate system (N) in which the chain may have N distinct configurations. The N frame is rigidly attached on

a molecule-fixed (M) frame with an orientation specified by the time-independent Euler angles Ω_{MN}. In each configuration, a C-D bond has a known orientation. Its motion due to conformational transitions is responsible for spin relaxation. Transitions between different configurations take place by means of one-bond, two-bond or three-bond motions [4.7, 4.8] in the chain. These bond motions involve jump rate constant k_1, k_2 and k_3, respectively. Transitions among configurations are described by a master equation [4.11]

$$\frac{\partial p_{il_0}(t)}{\partial t} = \sum_{j=1}^{N} R_{ij} p_{il_0}(t) \tag{4.11}$$

where R_{ij} is the rate constant for transitions from configuration j to configuration i and is related to the elementary jump rate constant r_{ij} which depends on the type of bond motion in the transition. r_{ij} is zero if transition cannot occur via one of the three types of bond motion. The diagonal matrix elements R_{ii} are the negative of the sum of all jump rates that deplete configuration i,

$$R_{ii} = -\sum_{j \neq i} R_{ji} \tag{4.12}$$

Moreover, R_{ij} satisfy the detailed-balance principle,

$$R_{ij} p_{eq}(j) = R_{ji} p_{eq}(i) \tag{4.13}$$

To construct the R matrix, it is required that $r_{ij} = r_{ji}$ and $R_{ij} = p_{eq}(i)\, r_{ij}$. The master equation can be solved [4.9] as a eigenvalue problem. This is achieved by symmetrizing R

and then diagonalizing to give N real and negative eigenvalues λ_n and eigenvectors $x^{(\vec{n})}$. One of these eigenvalues ($n = 1$) is zero, and the corresponding eigenvectors $x^{(\vec{1})}$ is given by the equilibrium distribution of configurations:

$$x_l^{(1)} = [p_{eq}(l)]^{1/2} \tag{4.14}$$

The conditional probability $P_{il_0}(t)$ is given by

$$P_{il_0}(t) = x_i^{(1)} \left(x_l^{(1)}\right)^{-1} \sum_{n=1}^{N} x_i^{(n)} x_l^{(n)} \exp(-|\lambda_n| t) \tag{4.15}$$

Now, applying the N frame coordinate system described above, and using the decomposition theorem for the Wigner matrix components, Eq. (4.1) can be rewritten as

$$D^2_{m_L 0}[\Omega_{LQ}(t)] = \sum_{m_M} \sum_{m_N} D^2_{m_L m_M}[\Omega_{LM}(t)] D^2_{m_M m_N}[\Omega_{MN}] D^2_{m_N 0}[\Omega_{NQ}(t)] \tag{4.16}$$

where the Euler angle Ω_{NQ} give the orientation of C-D bond in the N frame. Both Ω_{LM} and Ω_{NQ} are time dependent because of molecular reorientation and internal motion, respectively. Following the procedure of section 4.2, the decoupled model gives

$$\begin{aligned} G_{m_L}(t) \;=\; & \sum_{m_M} \sum_{m'_M} \sum_{m_N} \sum_{m'_N} D^2_{m_M m_N}[\Omega_{MN}] D^2_{m'_M m'_N}[\Omega_{MN}] \\ & \times g_{m_L m_M m'_M} \left\langle D^2_{m_N 0}[\Omega_{NQ}(0)] D^{2*}_{m'_N 0}[\Omega_{NQ}(t)] \right\rangle \\ & + \delta_{m_L 0} \langle P_2 \rangle^2 \sum_{m_N} \sum_{m'_N} \left\langle D^2_{m_N 0}[\Omega_{NQ}(0)] D^{2*}_{m'_N 0}[\Omega_{NQ}(t)] \right\rangle \end{aligned} \tag{4.17}$$

The internal correlation functions are given by

$$\begin{aligned}\left\langle D^2_{m_N 0}\left[\Omega_{NQ}(0)\right] D^{2*}_{m'_N 0}\left[\Omega_{NQ}(t)\right]\right\rangle &= \sum_{i,l} \exp\left(-im_N\alpha^l_{NQ}\right) d^2_{m_N 0}\left(\beta^l_{NQ}\right) p_{eq}(l) \\ &\quad \times \exp\left(-im'_N\alpha^i_{NQ}\right) d^2_{m'_N 0}\left(\beta^i_{NQ}\right) p_{il_0}(t) \\ &= \sum_{k=1}^{N} \exp\left(-|\lambda_k|t\right)\left[\sum_{l=1}^{N} x^{(1)}_l x^{(k)}_l \exp\left(-im_N\alpha^l_{NQ}\right) d^2_{m_N 0}\left(\beta^l_{NQ}\right)\right] \\ &\quad \times \left[\sum_{l'=1}^{N} x^{(1)}_{l'} x^{(k)}_{l'} \exp\left(-im'_N\alpha^{l'}_{NQ}\right) d^2_{m'_N 0}\left(\beta^{l'}_{NQ}\right)\right] \end{aligned} \tag{4.18}$$

where β^l_{NQ} and α^l_{NQ} are polar angles of a C-D bond in the rotamer of configuration l in the N frame, and Eq. (4.15) was substituted in the last step.

When applying TZ model to treat chain deuterons of an asymmetric rotor and letting $\Omega_{MN} = 0$ for simplicity, i.e., the N frame is coincident with the M frame, the spectral densities of C_i deuterons can be obtained for $m_L \neq 0$

$$\begin{aligned} J^{(i)}_{m_L}(m_L\omega) &= \frac{3\pi^2}{2}\left(q^{(i)}_{CD}\right)^2 \sum_{m_M}\sum_{m'_M}\sum_{k=1}^{N}\left[\sum_{l=1}^{N} x^{(1)}_l x^{(k)}_l \exp\left(-im_N\alpha^{(i)l}_{NQ}\right) d^2_{m_N 0}\left(\beta^{(i)l}_{NQ}\right)\right] \\ &\quad \times \left[\sum_{l'=1}^{N} x^{(1)}_{l'} x^{(k)}_{l'} \exp\left(-im'_N\alpha^{(i)l'}_{NQ}\right) d^2_{m'_N 0}\left(\beta^{(i)l'}_{NQ}\right)\right] \\ &\quad \times \sum_K \frac{\left(b^{22}_{m_L m_M m'_M}\right)_K \left[\left(a^{22}_{m_L m_M m'_M}\right)_K + |\lambda_k|\right]}{\left[\left(a^{22}_{m_L m_M m'_M}\right)_K + |\lambda_k|\right]^2 + (m_L\omega)^2} \end{aligned} \tag{4.19}$$

where a and b are defined in Eq. (3.26).

In this chapter we take the internal motion of the chain into account, and get the spectral densities for deuterons along a flexible chain.

References

[4.1] R. Y. Dong, Phys. Rev., A, **43**, 4310, 1991; R. Y. Dong and G. M. Richards, Chem. Phys. Lett., **171**, 389, 1990

[4.2] A. Ferrarini, G. J. Moro, P. L. Nordio, Liq. Cryst., **8**, 593, 1990

[4.3] P. A. Beckmann, J. W. Emsley, G. R. Luckhurst and D. L. Turner, Mol. Phys., **59**, 97, 1986

[4.4] P. J. Flory, "Statistical Mechanics of Chain Molecules", Inter-sciences, New York, 1969

[4.5] P. L. Nordio, P. Busolin, J. Chem. Phys., **55**, 5485, 1971

[4.6] P. L. Nordio, G. Rigatti and U. Segre, J. Chem. Phys., **56**, 2117, 1972

[4.7] B. Valeur, J. P. Jarry, F. Grny and L. Monnerie, J. Polym. Sci., **13**, 667, 1975

[4.8] B. Valeur, L. Monnerie, J. P. Jarry, J. Polym. Sci., **13**, 675, 1975

[4.9] R. Y. Dong and G. M. Richards, Chem. Phys. Lett., **200**, 541, 1992

[4.10] J. P. Caniparoli, A. Grassi and C. Chachaty, Mol. Phys., **63**, 419, 1988

[4.11] R. J. Wittebort and A. Szabo, J. Chem. Phys., **69**, 1722, 1978

5 Experimental Methods

5.1 Apparatus

A home-built superheterodyne coherent pulse NMR spectrometer was operated for deuterons at 15.1 MHz using a Varian electromagnet and at 46.05 MHz using a 7.1 Telsa Oxford superconducting magnet. The sample was placed in a NMR probe whose temperature was regulated either by an external oil bath circulator or by an air flow with a Bruker BST-1000 temperature controller. The temperature gradient across the sample was estimated to be less than 0.3 °C. The $\pi/2$ pulse width of about 4 μs was produced by a ENI power amplifier. Pulse control and signal collection were performed by a General Electric 1280 computer. Fourier transformation and data processing [5.1] were done by Spectral Calc and Micro Origin softwares on a IBM-PC computer. The temperatures in our samples were calibrated against a standard liquid crystal in which the transition temperatures are known and can be determined by NMR.

5.2 Quadrature Detection and Phase Cycling

Typically, a particular experiment is repeated many times and the output signals are summed before performing the Fourier transformation. This improves the signal to noise ratio. In a simple NMR experiment in which the signal from the sample is detected along

only one axis of the stationary reference frame, the excitation pulse must be placed either to the extreme left or to the extreme right of the spectrum, rather than near to the NMR line of interest, in order to avoid folding, or aliasing, of the NMR lines. In this case, the negative part of the spectrum is folded over and summed with the positive part of the spectrum. This causes the noise to double. Consider the Fourier transform of a single NMR line when the excitation pulse is placed relatively near to the line. The Fourier transform produces two peaks on either side of the excitation, one of the which is the real signal and the other is a fictitious signal. Also, since only one channel is used in the single phase detection, the detector sees only one magnetization component in the rotating frame and it is unable to tell if the magnetization is precessing faster ($\Delta\nu = \nu - \nu_0 > 0$) or slower ($\Delta\nu < 0$) than the excitation frequency.

To avoid spectrum folding, or aliasing, the quadrature detection method has been introduced [5.2, 5.3] . Using this technique, the FID signal from the sample is detected by two channels in a receiver which differ in phase by 90°. The signals in the two channels form a complex signal with certain amplitude and phase. This phase carries information that distinguishes signals having a positive offset from a negative offset. That is, nuclei that resonate at a frequency with $\Delta\nu > 0$ produce a different signal than nuclei that resonate at a frequency with $\Delta\nu < 0$. Thus the Fourier transformation of this signal produces spectrum which does not have the unwanted line and has the real line of double

the intensity. The signal to noise ratio is improved by a factor of $\sqrt{2}$ [5.4, 5.5].

The quadrature signals from the receiver are sent to two channels in the 1280 computer for signal averaging. Now the phase difference of the two channels in a receiver may deviate from the desired value of 90° and the gains of these channels may not be exactly the same. These problems are solved by using phase cycling of both radiofrequency pulses and the receiver channels. The computer controls the phase shifter to produce $r.f.$ phases at 0°, 90°, 180°, 270°. The receiver channels take turns in detecting the real and imaginary parts of the FID (Free Induction Decay) signal, as the receiver phase is cycled between 0° and 90°. As a result, the two channels equally share any error in quadrature or amplification. Then the computer collects the real and imaginary parts of the FID signal and sums them in two separate memories [5.5]. Thus the imperfection in $r.f.$ phases and in the quadrature detector of the receiver are compensated.

5.3 Pulse Sequence

In order to observe relaxation effects, the spin system has to be disturbed from equilibrium. In NMR this is usually done by applying an oscillating magnetic field for a short period. This oscillating field carries a frequency at or near the Larmor frequency ω_0 of the spin. The setup of a typical longitudinal relaxation experiment is shown in Fig.3.1. The shaded rectangle represents one or more $r.f.$ pulses. Their pulse length and inter-pulse spacing

determine the initial conditions of the spin system for the relaxation experiment. The spin system is left to relax during a period of t. A detection pulse is then applied to measure the spin magnetization along the Z_L axis by observing the time domain FID signal.

For deuterated liquid crystal molecules, the spin-lattice relaxation rates can be measured using the Jeener-Broekaert (J-B) pulse sequence with phase cycling as described by Vold *et al* [5.2, 5.3]. Note that the above pulse sequence has included an additional monitoring 45° pulse to minimize the long-term instability of the spectrometer. The pulse was phase-cycled to have a net effect of subtracting magnetization (M_0) signal from the J-B signal. After the spin system has been put in a non-equilibrium state by the first two pulses of the sequence, its relaxation to the equilibrium state is monitored by a detection pulse at various times t. The deuteron gives rise to a doublet, due to the incomplete averaging of the quadrupole coupling, and the intensity of the two lines of the doublet, here named L and H, depend on the time t as [5.6]

$$\begin{aligned} M_L &= A\exp(-t/T_{1Z}) - B\exp(-t/T_{1Q}) \\ M_H &= A\exp(-t/T_{1Z}) + B\exp(-t/T_{1Q}) \end{aligned} \tag{5.1}$$

where A and B are constants determined by the initial state of the system. By adding and subtracting M_L and M_H, respectively, the Zeeman and quadrupolar relaxation times T_{1Z} and T_{1Q}, can be obtained.

In our experiments, we use the broadband Jeener-Broekaert sequence (see Figure 3.2)

with the appropriate phase-cycling of radiofrequency and receiver phase [5.7] to simultaneously measure T_{1Z} and T_{1Q}. This avoids the necessity of matching the pulse separation between the first two pulses in the traditional J-B method to the quadrupolar splitting of the observed deuteron.

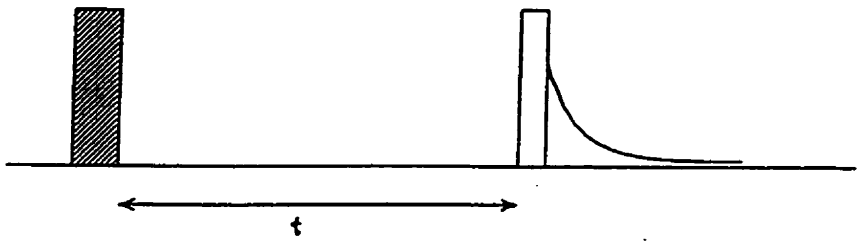

Figure 5.1 A schematic illustration of typical setup of a longitudinal relaxation experiment

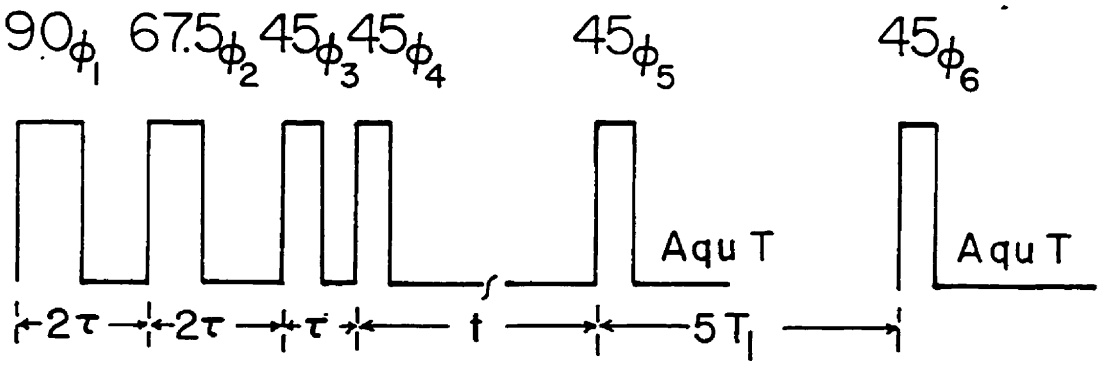

Figure 5.2 A schematic illustration of broadband Jeener-Broekaert sequence, ϕ_i specify the phases.

5.4 Liquid Crystal Samples

(1) MBPUB-d_2

S-4-(2-methylbutyloxy)carbonylphenyl1 4-(10-undecenyloxy)-benzoate

MBPUB-d_2 was kindly provided by Dr. C. A. Veracini, University of Pisa. This is a partially ring-deuteriated smectogen. It has a clearing temperature of 52.5 °C, SmA-SmC at 44 °C and a melting temperature of 43 °C. A broadband J-B excitation sequence [5.8] was used to measure simultaneously T_{1Z} and T_{1Q} of the aromatic deuterons. The pulse sequence was modified using an additional monitoring $\pi/4$ pulse to minimize any long term instability of the spectrometer. Signal collection was started 10 μs after each monitoring $\pi/4$ pulse, and averaged for over 1024 scans at 46 MHz and 4096 scans at 15.1 MHz. The experimental uncertainty in these spin-lattice relaxation times was estimated to be $\pm 5\%$. The quadrupolar and dipole splittings of the aromatic deuterons were determined from a NMR spectrum obtained by Fourier transforming the free induction decay signal after a $\pi/2$ pulse, and had an experimental error of better than $\pm 1\%$.

(2) 8OCB-d_{17}/6OCB mixture

4-n-octyloxy-4'-cyanobiphenyl (8OCB-d_{17})

4-n-hexyloxy-4'-cyanobiphenyl (6OCB)

The 8OCB-d_{17} was purchased from Merck, Sharp and Dohme Canada Ltd. in Montreal, and 6OCB was purchased from BDH Chemicals, Ltd. The 8OCB-d_{17}/6OCB mix-

ture has 72 wt% of 8OCB-d_{17} and 28 wt% of 6OCB. They were combined, melted thoroughly and evenly, degassed and sealed. The binary mixture has a clearing temperature of 79°C, N-SmA at 43°C and SmA-N_{re} at 32.5°C. A broadband J-B sequence [5.8] was used to simultaneously measure T_{1Z} and T_{1Q}. Signal collection was started 10 μs after each monitoring $\pi/4$ pulse, and averaged over 4096 scans at 46 MHz and 8192 scans at 15.1 MHz. The experimental uncertainty in these spin-lattice relaxation times was estimated to be ±5%. Quadrupolar splittings were determined from a NMR spectrum obtained by Fourier Transform of the free induction decay signal after a $\pi/2$ pulse, and had an experimental error of better than ±1%.

References

[5.1] R. Y. Dong and G. M. Richards, J. Chem. Soc. Faraday Trans. II **84**, 1053, 1988

[5.2] R. L. Vold, W. H. Dickerson and R. R. Vold, J. Magn. Reson., **43**, 213, 1981

[5.3] T. M. Barbara, R. L. Vold and R. R. Vold, J. Magn. Reson., **59**, 478, 1984

[5.4] E. O. Stejskal and J. Schaefer, J. Magn. Reson., **13**, 249, 1974; ibid **14**, 160, 1974

[5.5] Eiichi Fukushima and Stephen B. W. Roeder, "Experimental Pulse NMR", Addison-Wesley Publishing Company, Inc., 1981; GN-Series Software Manual, General Elec-

tric, 1991

[5.6] R. Y. Dong, "Nuclear Magnetic Resonance of Liquid Crystal", Spring-Verlag, N. Y., 1997

[5.7] R. Y. Dong, Bull of Magn. Reson., **14**, 134, 1992; S. Wimperis, J. Magn. Reson., **86**, 46, 1990

[5.8] S. Wimperis, J. Magn. Reson., **83**, 590, 1990; **86**, 46, 1989

6 Rotational Dynamics of a Chiral Mesogen

6.1 Introduction

Chiral molecules used to form ferro- and antiferro-electric liquid crystals have recently attracted much attention owing to the observation of a rich variety of chiral subphases [6.1, 6.2]. Indeed chirality is now thought of to be an important element in creating novel organizations and functions of liquid crystalline materials. Molecular chirality can be created by placing asymmetric carbons in the end chain(s) of a non-chiral liquid crystal molecule. There is now evidence that a chiral chain is motionally hindered in the liquid crystalline phase, as the chain is bent at the chiral centre with respect to the molecular long axis [6.3 – 6.6]. A bent shape increases the molecular biaxiality and the moment of inertia. This is consistent with the belief that in order to see macroscopic polarization, rotation around the molecular long axis must be highly restricted. NMR studies of conventional rod-like mesogens have clearly established that the spinning motion (around the molecular long axis) of the molecule is about two orders of magnitude faster than its tumbling motion (around one of the short axis) [6.7]. In the present study, the molecule of an optically pure chiral mesogen is found to show rotational behaviors which may be anomalous.

Our sample, MBPUB-d_2, was studied by deuterium NMR spectroscopy. A typical spectrum of MBPUB-d_2 is shown in Fig. 6.1 together with its chemical structure. The

permanent dipoles are located mainly on the two carbonyl groups in the molecule and pointed approximately perpendicular to the molecular long axis.

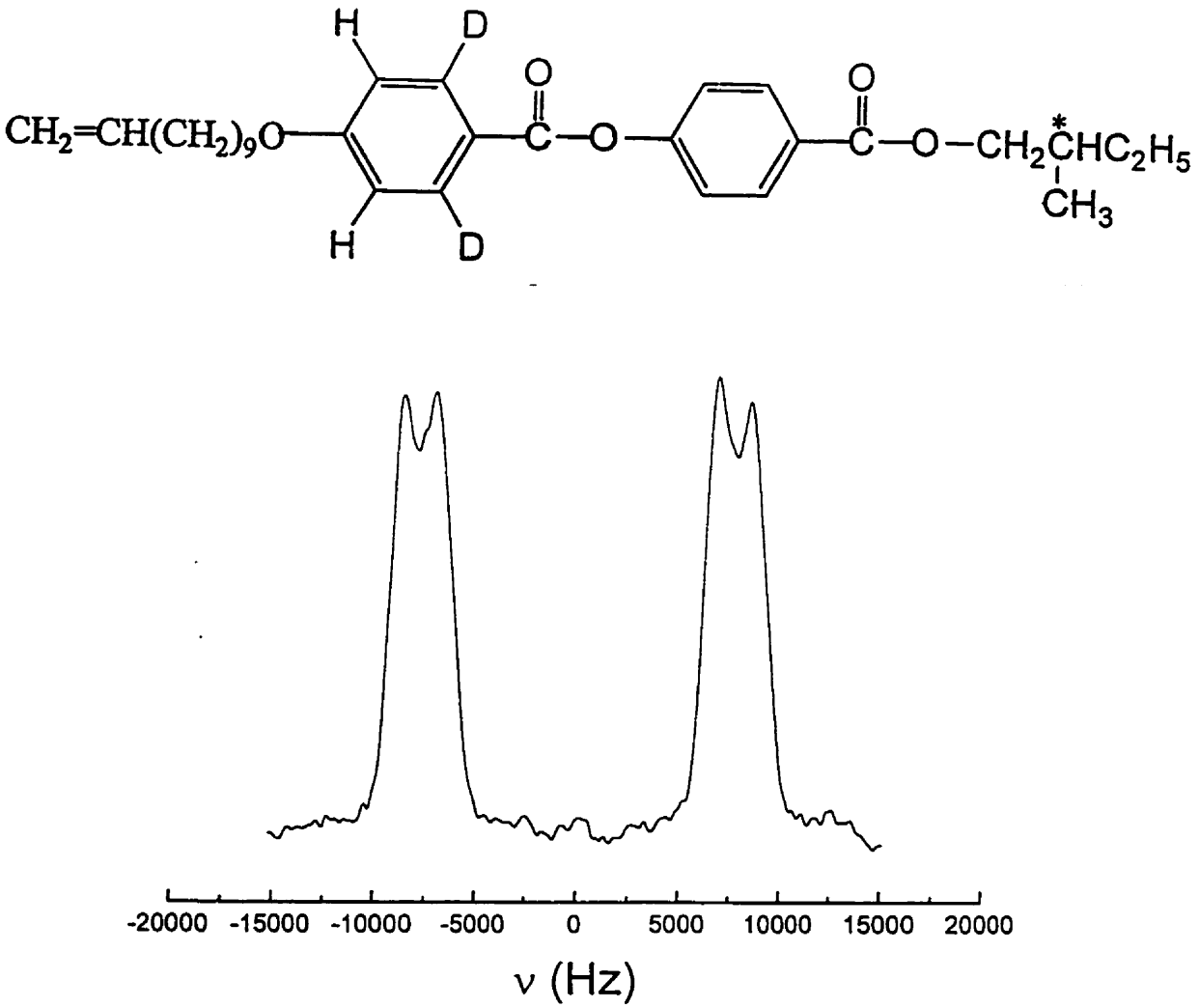

Figure 6.1 A typical DMR spectrum of MBPUB-d_2 and its molecular structure

Although MBPUB has a narrow one degree range of SmC* phase, our sample only shows the SmA phase with an extended temperature range by supercooling. As seen in Figure 6.1, the spectrum consists of a quadrupolar doublet (with a splitting $\Delta\nu_Q$) whose peaks shows an additional splitting ($\Delta\nu_D$) due to the dipole-dipole coupling between the deuteron and its nearby proton. The observed splittings are a result of the anisotropic motion of molecules within fluid layers in the SmA phase. The splittings $\Delta\nu_Q$ and $\Delta\nu_D$ datas versus temperature at 46 MHz are shown in Figure 6.2. It is clear from this figure that the data show some temperature dependence.

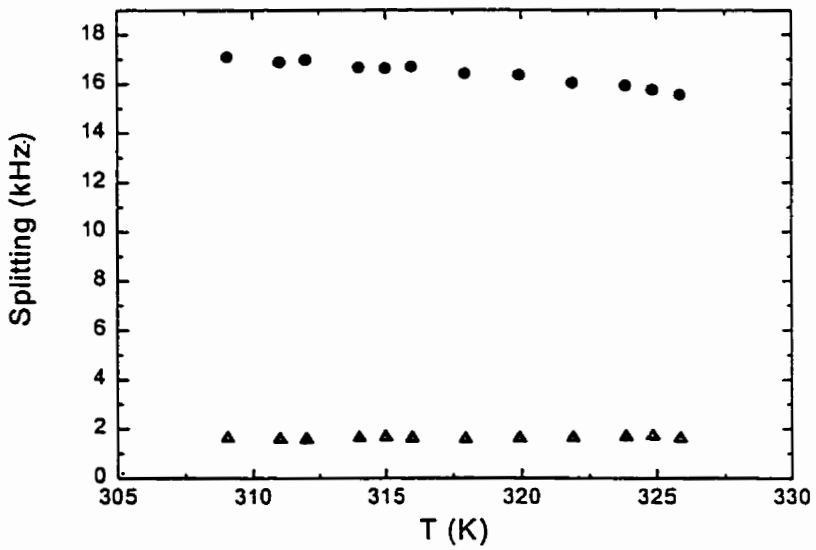

Figure 6.2 Plot of quadrupolar splittings $\Delta\nu_Q$ and dipolar splittings $\Delta\nu_D$ versus the temperature at 46 MHz. Circles and up triangles denote $\Delta\nu_Q$ and $\Delta\nu_D$, respectively.

6.2 Data Analysis

In a previous study [6.10], the para axes of the phenyl rings in MBPUB were found to make an angle of 12°. We estimate that the molecular z_M axis makes an angle $\theta = 6°$ with the para axis of the deuterated ring. Using the $\Delta\nu_Q$ and $\Delta\nu_D$ from Eqs. (2.20) and (2.22), the principal values $P_2 (= S_{zz})$ and $S_{xx} - S_{yy}$ of the order parameter matrix of the molecule core can be determined at each temperature according to:

$$\Delta\nu_Q = -\frac{3}{8} q_{CD} \left[P_2 f(\theta) - \frac{1}{2} (S_{xx} - S_{yy}) g(\theta) \right] \tag{6.1}$$

$$\Delta\nu_D = -2K_{DH} \frac{1}{r_{DH}^3} \left[P_2 \left(\frac{3}{2} \cos^2\theta - \frac{1}{2} \right) - \frac{1}{2} (S_{xx} - S_{yy}) \sin^2\theta \right] \tag{6.2}$$

where q_{CD} (185 kHz) is the nuclear quadrupolar coupling constant. K_{DH} (18.434 kHz Å^3) is the D-H dipolar coupling constant, r_{DH} (2.5 Å) is the proton-deuteron distance, and the functions [6.11] $f(\theta) = 3\sin^2\theta + \eta\cos^2\theta + (\eta - 1)/2$ and $g(\theta) = 1 + 2\cos^2\theta + \eta(5 + 2\sin^2\theta)/3$. In Eq. (6.1), a normal value of $\theta_{R,Q} = 60°$ for the angle between the C-D bond and the para axis, and an average of quadrupolar splittings from the two non-equivalent C-D bonds in the (x_M, y_M, z_M) frame has been used. Also, $\eta = 0.04$ is assumed. The derived order parameters are shown in Figure 6.3. These are used to construct the orienting pseudopotential for the spin relaxation study. As seen in the Figure 6.3, the molecular biaxiality $(S_{xx} - S_{yy})$ is small (*ca.*0.03) and the nematic order parameter P_2 (*ca.*0.7) increases very slightly over the entire SmA phase upon decreasing

temperature.

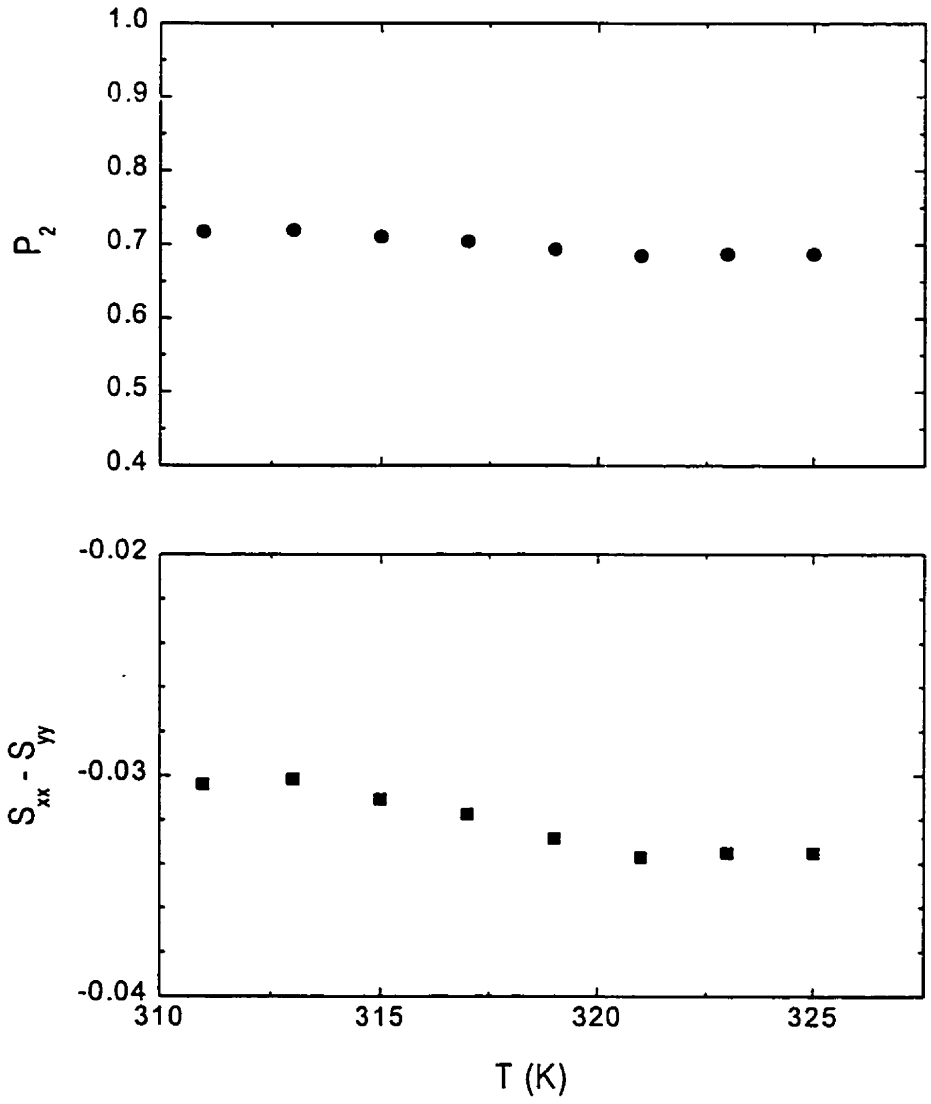

Figure 6.3 Plots of order parameters P_2 and $S_{xx} - S_{yy}$ versus the temprature

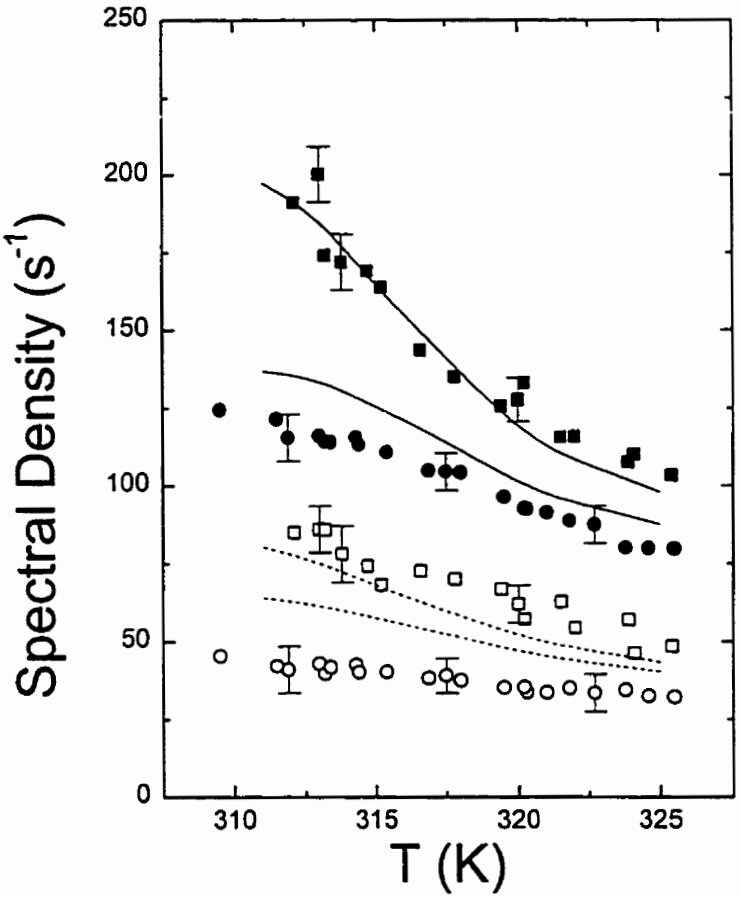

Figure 6.4 Plot of spectral densities versus the temperature. Closed and open symbols denote $J_1(\omega)$ and $J_2(2\omega)$ respectively. Squares and circles denote data collected at 15.1 and 46 MHz, respectively. Solid and dashed lines denote calculated spectral densities at 15.1 and 46 MHz, respectively.

The spectral densities $J_1(\omega)$ and $J_2(2\omega)$ are shown in Figure 6.4. We found that both J_1 and J_2 show strong frequency dependences, and increase with decreasing temperature in the SmA phase. The apparently large frequency dependence in J_2 cannot be explained by the well-known relaxation mechanism called director fluctuations (ODF) [6.7]. Furthermore, the ring deuteron is known to be insensitive to the ODF because of the orientation of its C-D bond being close to the magic angle. We therefore ignore any contributions from the ODF and choose to explain our spectral density data using the small-step rotational diffusion model of Nordio [6.12], but with a minor modification [6.13] for a (molecular) biaxial orienting potential. We note that the rotational diffusion tensor is diagonal in (x_M, y_M, z_M) frame with principal values $D_{zz}(= D_{\parallel})$ and $D_{xx} = D_{yy}(= D_{\perp})$. Internal ring rotations about its para axis and the overall motion of the molecule are assumed to be uncorrelated so that the superimposed rotation model [6.14] is used. Furthermore, ring rotations with a rotational diffusion constant D_R may be treated either in the small step diffusive limit [6.15] or in the strong collision limit [6.14]. Using the notation of Tarroni and Zannoni [6.13], the ring deuteron spectral density is given by Eq. (3.30). Using an Arrhenius temperature dependence for three model parameters, gives:

$$D_{\perp} = D_{\perp}^{\circ} \exp\left(-E_a^{D_{\perp}}/RT\right) \tag{6.3}$$

$$D_{\parallel} = D_{\parallel}^{\circ} \exp\left(-E_a^{D_{\parallel}}/RT\right) \tag{6.4}$$

$$D_R = D_R^{\circ} \exp\left(-E_a^{D_R}/RT\right) \tag{6.5}$$

where $D_{\perp}^{\circ}$, $D_{\parallel}^{\circ}$ and D_{R}° are the pre-exponentials, and their corresponding activation energies are $E_a^{D_{\perp}}$, $E_a^{D_{\parallel}}$ and $E_a^{D_R}$, respectively.

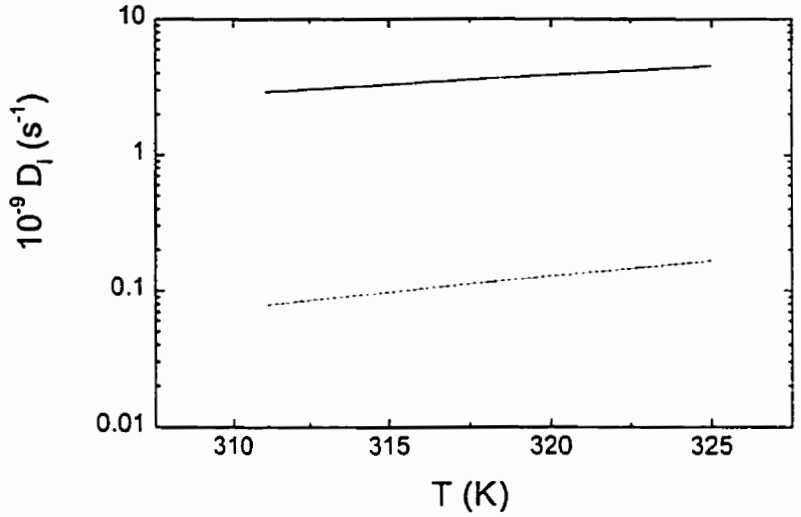

Figure 6.5 Plot of rotational diffusion constants versus the temperature. Solid, dash-dotted and dotted lines denote $D_{\perp}$, D_R and $D_{\parallel}$ respectively.

A global analysis of eight different temperatures was carried out to minimize the sum square deviation of experimental and calculated spectral densities with AMOEBA [6.16]. Because the correlation coefficient between the pre-exponential and its corresponding activation energy is as high as 0.99 [6.8], we rewrite Eqs. (6.3) – (6.5) in terms of $D'_{\perp}$, $D'_{\parallel}$ and D'_R at $T_{\max} = 325K$, the highest temperature used in the global analysis. Thus

six target parameters ($D'_{\perp}$, $D'_{\parallel}$, D'_R and three activation energies) were varied in the minimization. The quality factor Q is defined by

$$Q = \frac{\sum_k \sum_m \sum_i \left[J_m^{calc}(m\omega_i) - J_m^{\exp}(m\omega_i)\right]_k^2}{\sum_k \sum_m \sum_i \left[J_m^{\exp}(m\omega_i)\right]_k^2} \tag{6.6}$$

where k is summed over eight temperatures, sum over m is for 1 and 2, and i is for two frequencies. Again the calculated spectral densities are again shown in Figure 6.4, and the derived model parameters are shown in Figure 6.5, with a $Q = 1.3\%$. Despite the relatively small Q value, there are systematic deviations between the experimental and calculated spectral densities, especially in $J_2(2\omega)$ and at low temperatures. These deviations are largely due to limitations of the adopted motional model. We note that the tumbling motion ($D_{\perp}$) is faster than spinning motion ($D_{\parallel}$) which is a surprise. That $D_{\parallel}$ and D_R values are found to be comparable seems to follow other non-chiral rodlike mesogens. The slow spinning rate ($ca.10^8 s^{-1}$) may stem from the bent shape of the molecule and its larger moment of inertia about the long axis. Similar spinning rates have been reported in the SmA phase of other chiral compounds by dielectric spectroscopy [6.9]. The activation energies $E_a^{D_{\perp}}$, $E_a^{D_{\parallel}}$ and $E_a^{D_R}$ are equal to 26.7 kJ/mol, 40.3 kJ/mol and 45.0 kJ/mol, respectively. The error limit of $E_a^{D_{\perp}}$ is ± 0.05 kJ/mol, while that of $E_a^{D_{\parallel}}$ varies between (44.7-38.5) kJ/mol and that of $E_a^{D_R}$ is (47.9-43.4) kJ/mol. For a particular target parameter, the error limit was estimated by varying the one under consideration

to give an approximate doubling the Q value while keeping all other target parameters identical to those for the minimum Q. The pre-exponentials $D_{\perp}^{\circ}$, $D_{\parallel}^{\circ}$ and D_{R}° are given by $8.74 \times 10^{13} s^{-1}$, $3.37 \times 10^{14} s^{-1}$, $2.84 \times 10^{15} s^{-1}$, respectively. These parameters represent reasonable "collision" frequencies for the different motional processes. The error limit for $D_{\perp}^{\circ}$ is $(1.08 - 0.71) \times 10^{14} s^{-1}$, for $D_{\parallel}^{\circ}$ is $(6.8 - 0.7) \times 10^{14} s^{-1}$, and for D_{R}° is $(5.3 - 0.95) \times 10^{15} s^{-1}$ [6.17].

References

[6.1] J. W. Goodby, J. S. Peter and E. Chin, J. Mater. Chem., **2**, 197, 1992

[6.2] M. Škarabot, M. Čepič, B. Žekš, R. Blinc, G. Heppke, A. V. Kityk and I. Muševič, Phys. Rev. E, **58**, 575, 1998

[6.3] S. Yoshida, B, Jin, Y. Takanishi, K. Tokumaru, K. Ishikawa, H. Takezoe, A. Fukuda, T. Kusumoto, T. Nakai and S. Miyajima, J. Phys. Soc. Japan, **68**, 9, 1999

[6.4] T. Nakai, S. Miyajima, Y. Takanishi, S. Yoshida and A. Fukuda, J. Phys. Chem., B, **103**, 406; K. Miyachi, Y. Takanishi, K. Ishikawa, H. Takezoe and A. Fukuda, Phys. Rev. E, **55**, 1632, 1997

[6.5] Y. Ouchi, Y. Yoshioka, H. Ishii, K. Seki, M. Kitamura, R. Noyori, Y. Takanishi and I. Nishiyama, J. Mater. Chem., **5**, 2297, 1995

[6.6] B. Jin, Z. Ling, Y. Takanishi, K. Ishikawa, H. Takezoe, A. Fukuda, M. Kakimoto and T. Kitazume, Phys. Rev., E, **53**, R4295, 1996

[6.7] R. Y. Dong, "Nuclear Magnetic Resonance of Liquid Crystals", Spinger-Verlag, N.Y., 1997

[6.8] L. Calucci, M. Geppi, C. A. Veracini and R. Y. Dong, Chem. Phys. Lett., **296**, 357, 1988

[6.9] A. Schönfeld, F. Kremer and R Zentel, Liq. Cryst., **13**, 403, 1993; B. Gestblom, M. Makrenek, W. Hasse and S. Wróbel, Liq. Cryst., **14**, 1069, 1993

[6.10] D. Catalano, E. Chiellini, L. Chiezzi, K. Fodor-Csorba, G. Galli, E. Gacs-Baitz, S. Holly and C. A. Veracini, Mol. Cryst. Liq. Cryst. (in press)

[6.11] R. Y. Dong, G. S. Bates and X. Shen, Mol. Cryst. Liq. Cryst., **331**, 143, 1999

[6.12] P. L. Nordio and P. Busolin, J. Chem. Phys., **55**, 5485, 1997; P. L. Nordio, G. Rigatti and U. Segre, J. Chem. Phys., **56**, 2117, 1972

[6.13] R. Tarroni and C. Zannoni, J. Chem. Phys., **95**, 4550, 1991

[6.14] P. A. Beckmann, J. W. Emsley, G. R. Luckhurst and D. L. Turner, Mol. Phys., **54**, 97, 1986

[6.15] D. E. Woessner, J. Chem. Phys., **36**, 1, 1962

[6.16] W. H. Press, B. P. Flannery, S. A. Teukolsky and W. T. Vetterling, "Numerical Recipes", Cambridge, UK, 1986

[6.17] R. Y. Dong and M. Cheng, Liq. Cryst., (in press)

7 Molecular Dynamics in a Mixture of 8OCB-d_{17} and 6OCB

7.1 Introduction

NMR spectra of deuterated liquid crystals show well-resolved quadrupolar doublets. Hence, T_{1Z} (Zeeman) and T_{1Q} (Quadruplar) can be simultaneously determined for different atomic sites. From these T_1's, the extraction of spectral densities $J_1(\omega_0)$ and $J_2(2\omega_0)$ are possible, where $\omega_0/2\pi$ is the Larmor frequency. The additive potential(AP) method is employed to construct the potential of mean torque by modeling the quadrupolar splittings in the sample. A decoupled model is used to describe correlated internal motions of the end chain, which are assumed to be independent of the molecular reorientation. The latter motion is treated using the small-step rotational diffusion model of Tarroni and Zannoni ($D_x = D_y = D_\perp$ is used), while the former motion is described using a master rate equation. The experimental results were analyzed using the global target minimization approach [7.1] in order to obtain more reliable fitting parameters.

Our sample is a 72% 8OCB-d_{17} and 28% 6OCB mixture by weight. The 8OCB-d_{17} molecule is schematically shown in Fig. 7.1(a) and the peak assignment of a representative spectrum for the 8OCB-d_{17}/6OCB sample is shown in Fig. 7.1(b).

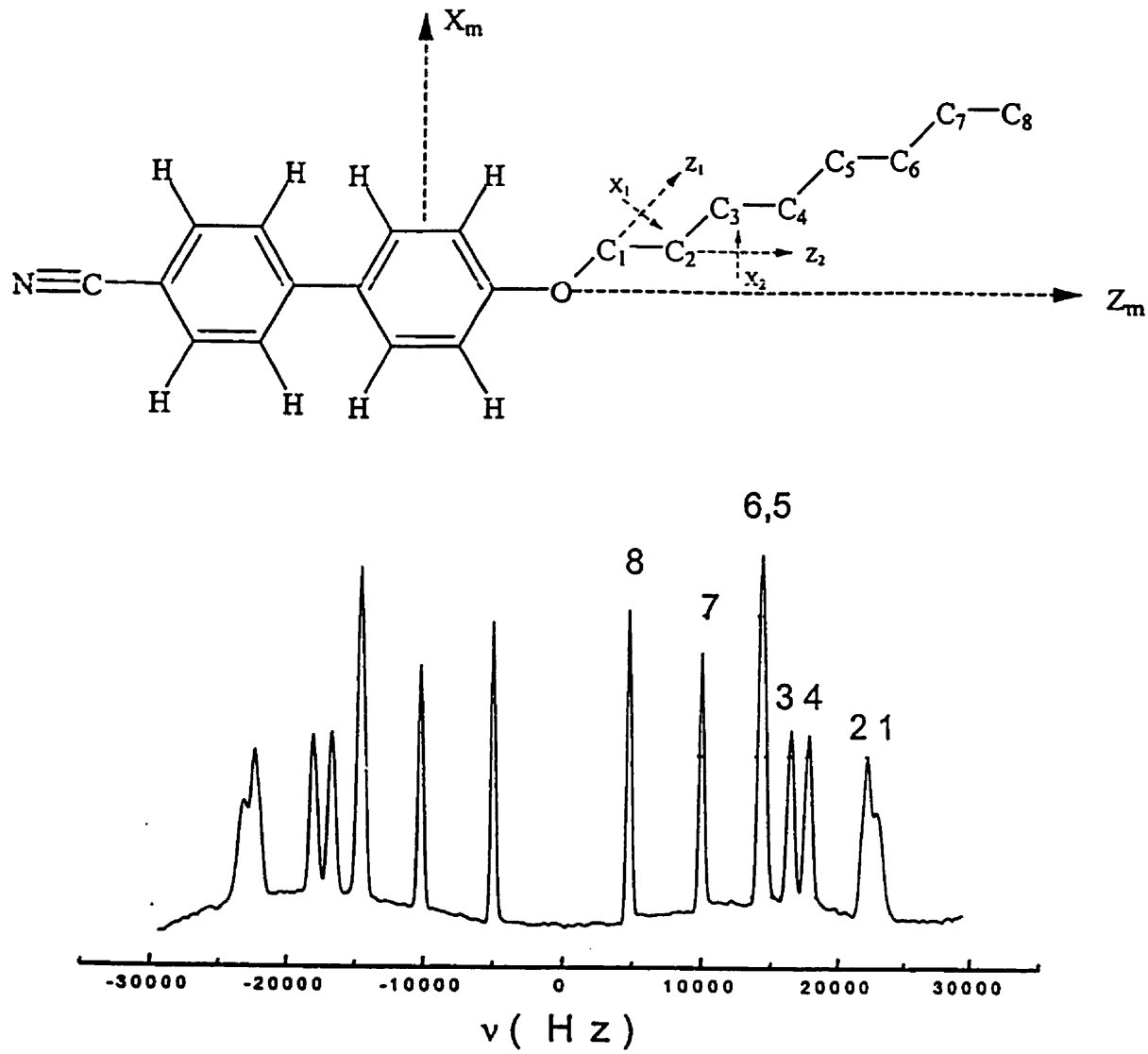

Figure 7.1 (a). Schematic diagram of a 8OCB-d_{17} molecule and various coordinate systems used. (b). A typical deuteron spectrum of 8OCB-d_{17} or 8OCB-d_{17}/6OCB mixture showing the peak assignment

The peaks from C_1 and C_2, and those from C_5 and C_6 did overlap, but deconvolution of the peaks for the individual carbon's deuterons was carried out whenever possible, noting the proper lineshapes of coupled deuteron pairs [7.4] . This allowed separate determination of relaxation times for the carbon sites in question. At 15.1 MHz, the peaks 1 and 2 could not be resolved by deconvolution at low temperatures, and the DMR signals of these carbon sites for relaxation measurements were obtained by simply integrating the areas in different parts of the overlapped (broad) line.

7.2 Data Analysis

The molecular mean field theory based on the additive potential (AP) method, the decoupled model and the small-step rotational diffusion model for biaxial probes have been presented in the previous chapters. The geometry used to describe the carbon-carbon backbone of an alkyloxy chain is adopted as [7.5]: $\angle CCC$ =113.5°, $\angle CCH$ =107.5° and $\angle HCH$ =113.6° . The dihedral angles for rotation to the *trans* (t) and two symmetric *gauche* ($g^{\pm}$) states are 0, ±112 °. The *gauche* states have higher internal energy in comparison to that of *trans* state by an amount of E_{tg}. The O-C_1 bond is fixed on the phenyl ring plane [7.6]. Using the pentane effect to eliminate any conformer which contains either a g^+g^- or g^-g^+ linkage, the number of conformations in the chain is 577 (i.e., $N_{g^{\pm}g^{\mp}} = 0$ in Eq. (2.30)).

It is known that the $\angle COC$ which specifies the direction of the chain relative to the molecular core plays an important role in the observed variations of segmental order and spin relaxation profiles. Thus $\angle COC = 126.4°$ was adopted [7.7]. The molecular core, which includes the first C_{ar}-O bond in the chain is assumed to be a rigid subunit and has cylindrical symmetry with an interaction parameter X_a. As an approximation, the bond interaction parameter of the O-C_1 bond is identical to those of C-C bonds, i.e., $X_{cc} = X_{oc}$. According to the model prediction [7.8], the ratio $\lambda_c = X_{cc}/X_a$ should be independent of temperature. The rotational minima about the O-C_1 bond of the hexyloxy chain were also taken to be 0, $\pm 112°$.

Figure 7.2 shows the experimental segmental order parameter $S_{CD}^{(i)}$ for 8OCB-d_{17} as a function of temperature in the N, SmA and N_{re} phases of the 8OCB/6OCB mixture. An optimization routine (AMOEBA) was used [7.9] to minimize the sum squared error f in fitting the experimental $S_{CD}^{(i)}$

$$f = \sum_i \left(\left| S_{CD}^{(i)} \right| - \left| S_{CD}^{(i)Calc} \right| \right)^2 \tag{7.1}$$

where $S_{CD}^{(i)Calc}$ is obtained from Eq. (2.28) with Eqs. (2.37)-(2.42) and the sum over i includes only the methylene deuterons in C_1 to C_7. The f values at different temperatures were found to be of the order of 10^{-3}. The calculated segmental order parameters are also indicated in Figure 7.2 as solid curves.

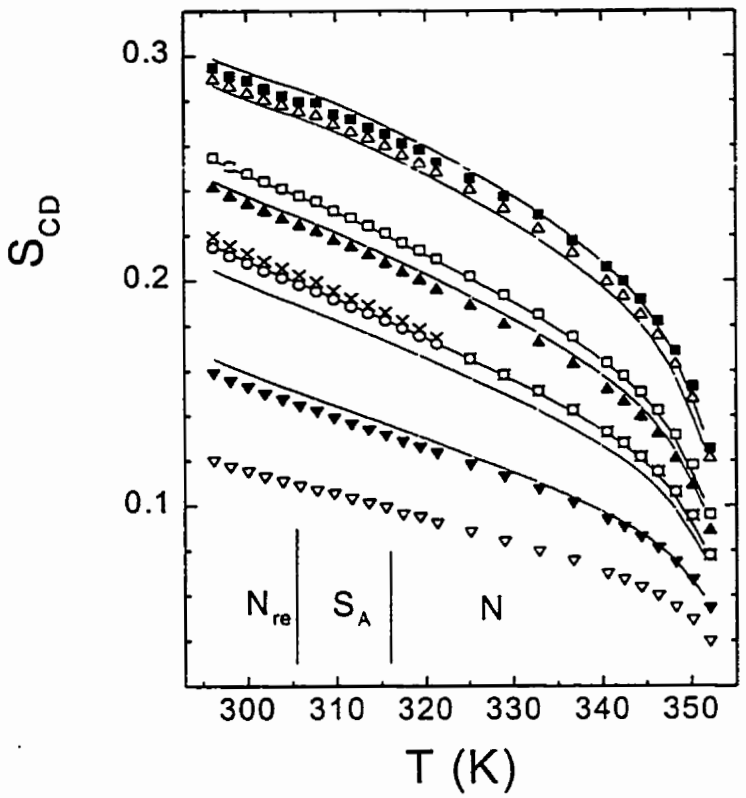

Figure 7.2 Plot of segmental order parameters of 8OCB in 8OCB/6OCB versus the temperature. Solid squares, uptriangles, × and downtriangles denote C_1, C_3, C_5 and C_7, respectively. Open uptriangles, squares, circles and downtriangles denote C_2, C_4, C_6 and C_8, respectively. The solid curves are the theoretical calculations for C_1 to C_7 starting from the top. Note that the experimental splittings of C_3 to C_4 are reversed from those predicted by the theory

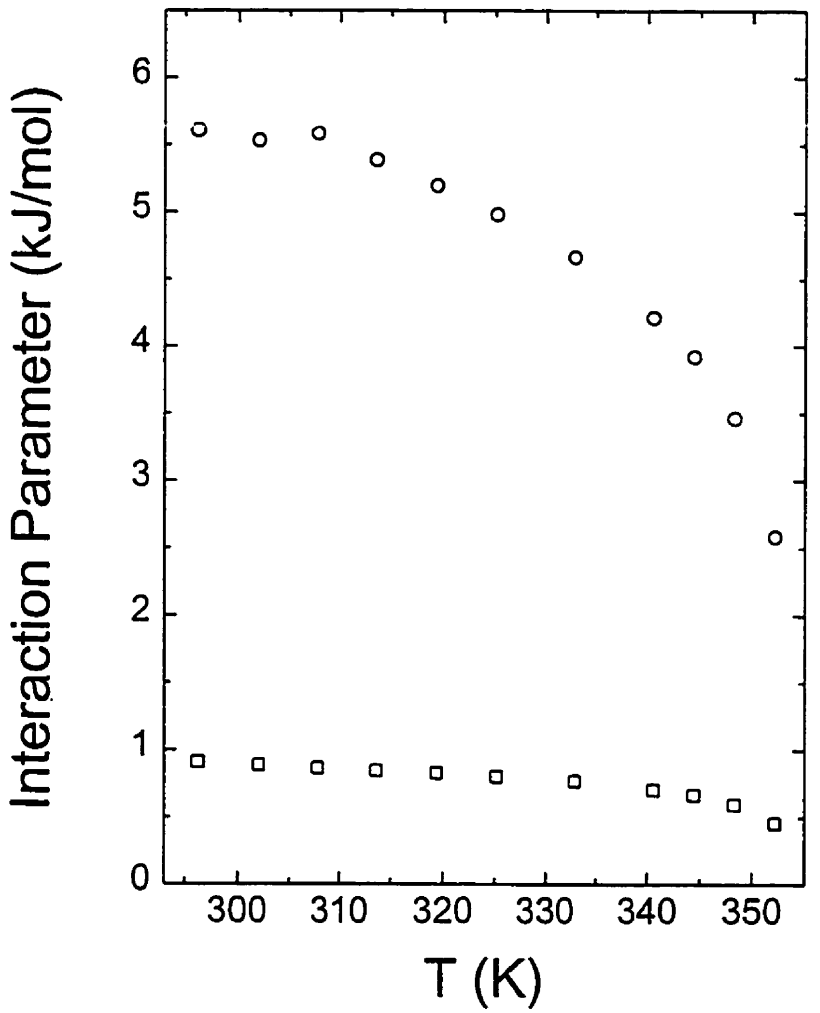

Figure 7.3 Plot of interaction parameters X_{cc} (square) and X_a (circle) versus the temperature

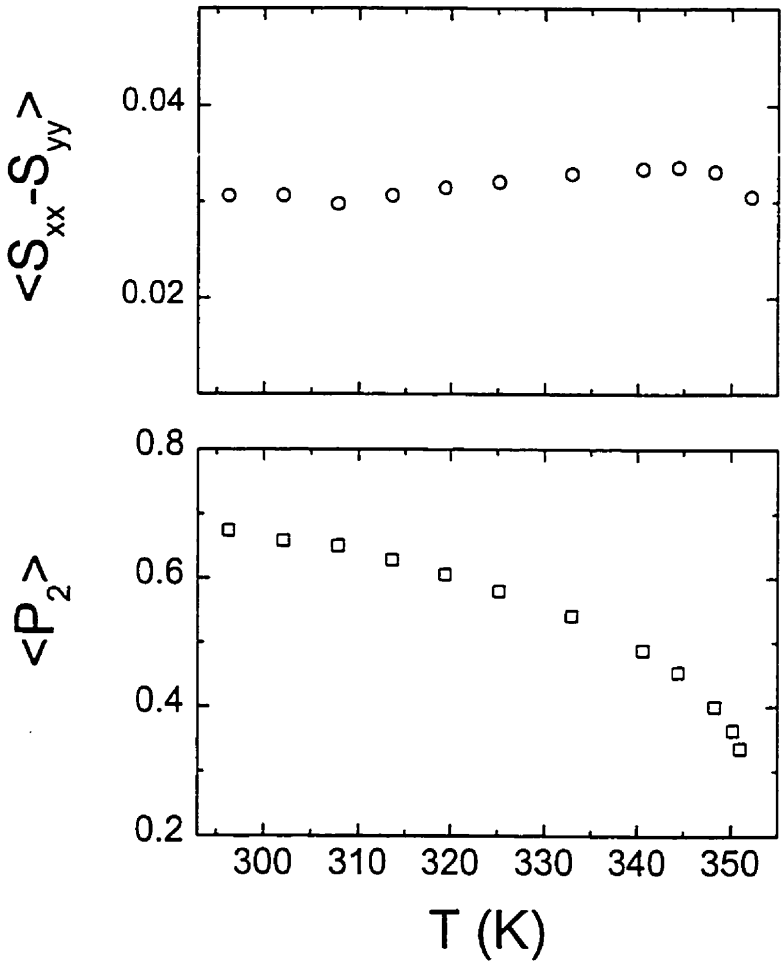

Figure 7.4 Plots of the order parameters $\langle P_2 \rangle$ and $\langle S_{xx} - S_{yy} \rangle$ of an "average" conformer of 8OCB in 8OCB/6OCB as a function of temperature

The tentative assignment of $\Delta\nu_3 < \Delta\nu_4$ cannot be reproduced by the AP method. In working out $U_{int}(n)$, $E_{tg}(CCC) = 4000$ J/mol and $E_{tg}(OCC) = 5600$ J/mol are

those used before for 8OCB [7.2]. The derived interaction parameters X_a and X_{cc} versus temperature in Figure 7.3 are comparable to those found in 6OCB and 8OCB. The interaction parameters found from fitting the quadrupolar splittings are then used to find $P_{eq}(n)$ needed in calculating the autocorrelation functions for internal motions of the chain. Furthermore, the order matrix of an "average" conformer of 8OCB has been evaluated at each temperature. Figure 7.4 shows its principal elements $\langle P_2 \rangle$ and $\langle S_{xx} - S_{yy} \rangle$ as a function of temperature, from these the coefficients a_{20} and a_{22} in Eq. (A.1) are obtained. Despite the obvious deviations between calculated and observed segmental order parameters in Figure 7.2, the resulting $P_{eq}(n)$, a_{20} and a_{22} are quite satisfactory for treating our relaxation data in all the mesophases.

The spectral density $J_1(\omega)$ and $J_2(2\omega)$ data versus the temperature for all the chain deuterons are shown in Figure 7.5 for 15.1 and 46 MHz. It is clear from this figure that $J_1^{(i)}(\omega)$ show substantial frequency dependences at all carbon sites, while $J_2^{(i)}(2\omega)$ shows less frequency dependences. In a study of 6OCB [7.10], similar frequency behaviors of the spectral density data in its nematic phase were accounted for only by the relatively "slow" molecular reorientation. Our results indicate that "slow" molecular reorientations can describe the frequency dependences of $J_1^{(i)}(\omega)$ and $J_2^{(i)}(2\omega)$ in the SmA and N_{re} phases, while some ODF contributions appear to be necessary in the high temperature N phase of the mixture.

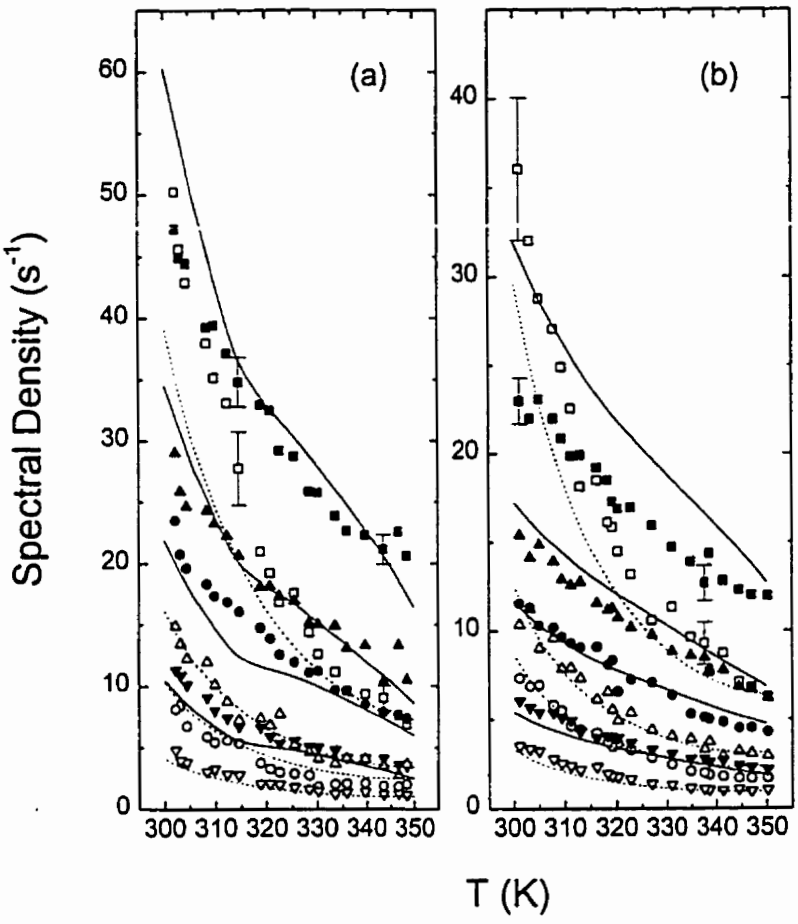

Figure 7.5 (a), (b) Plots of spectral densities versus temperature in 8OCB/6OCB at 15.1 MHz (Fig. (a)) and 46 MHz (Fig. (b)). Closed symbols denote $J_1^{(i)}(\omega)$ and open symbols denote their corresponding $J_2^{(i)}(2\omega)$. Squares, uptriangles, circles and downtriangles denote data of C_1, C_3, C_5 and C_7, respectively; Some typical error bars are shown. Solid and dashed curves denote calculated spectral densities J_1 and J_2, respectively

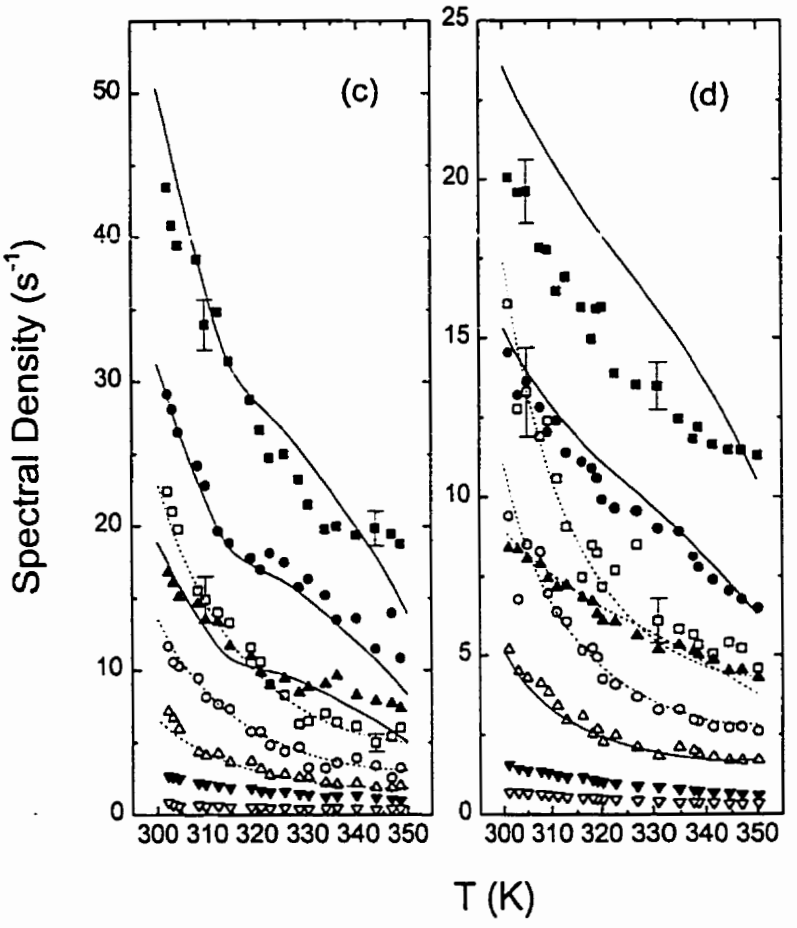

Figure 7.5 (c), (d) Plots of spectral densities versus temperature in 8OCB/6OCB at 15.1 MHz (Fig. (c)) and 46 MHz (Fig. (d)). Closed symbols denote $J_1^{(i)}(\omega)$ and open symbols denote their corresponding $J_2^{(i)}(2\omega)$. Squares, circles, uptriangles and downtriangles denote data of C_2, C_4, C_6 and C_8, respectively; Some typical error bars are shown. Solid and dashed curves denote calculated spectral densities J_1 and J_2, respectively

Since the motional biaxiality is believed to be small, we have set $D_x = D_y = D_\perp$. The spectral densities $J_1^{(i)}(\omega)$ and $J_2^{(i)}(2\omega)$ for carbon 1 to carbon 7 are calculated using Eqs. (3.41) and (4.19) and compared with their experimental values from all mesophases in a global target analysis. To get some ideas on the temperature behaviours of model parameters $D_\perp$, $D_\parallel$, k_1, k_2 and k_3, individual target analyses (i.e., analyze spectral densities at each temperature) were first carried out. These analyses have indicated that the target model parameters vary smoothly with temperature, even across different transitions. Furthermore, we found that the rotational diffusion constants obeyed simple Arrhenius relations:

$$\begin{aligned} D_\perp &= D_\perp^\circ \exp\left[-E_a^{D_\perp}/RT\right] \\ D_\parallel &= D_\parallel^\circ \exp\left[-E_a^{D_\parallel}/RT\right] \end{aligned} \tag{7.2}$$

while all jump constants showed weak temperature behaviours which might be approximated by

$$k_i = k_i' + k_i''(T - T_{ref}) \tag{7.3}$$

where $i = 1, 2$ or 3 and T_{ref} is arbitrarily chosen at 320 K. The pre-exponentials $D_\perp$, $D_\parallel$ and their corresponding activation energies $E_a^{D_\perp}$ and $E_a^{D_\parallel}$ are the global parameters. Similarly k_1', k_1'', k_2', k_2'', k_3' and k_3'' are the remaining global parameters in our global target analysis. Instead of Eq. (7.2), this was rewritten in terms of the activation energies and

the diffusion constants $D'_{\perp}$ and $D'_{\parallel}$ at T_{ref}. Indeed k'_1, k'_2, k'_3, $D'_{\perp}$ and $D'_{\parallel}$ were first obtained at 320 K by an individual target analysis. Now the ODF prefactor A was chosen by varying it as an input to give the "best" minimization of the mean-squared percent deviation (F) with AMOEBA. Thus, A was set equal to $6.7\times10^{-6}s^{1/2}$, while a linear temperature dependence was imposed for the high frequency cutoff ($\omega_c/2\pi$ = 90 MHz at 350 K) such that its value decreased to 3 MHz just below the N-SmA phase transition at 315 K. In this manner, the cutoff function $\Im(x)$ approaches 0 in the SmA phase. The choice of 90 MHz for the high frequency cutoff at 350 K seems quite reasonable in the overall fits of our experimental data. We found that ODF contribute at 15.1 MHz about 1.4-2.4% to $J_1^{(i)}(\omega)$ just below the N-SmA transition (315 K), and make zero contribution to $J_1^{(i)}(\omega)$ at lower temperatures. At the high end of the N phase (350 K), ODF contribute to $J_1^{(i)}(\omega)$ between 27% and 36% at 15.1 MHz (about 12-16% at 46 MHz). The ODF contributions, when compared with those in the pure 8OCB sample at the same temperature, are slightly higher. Although $J_{2ODF}^{(i)}$ were included here, their magnitudes were very small (e.g., <1% at 15.1 MHz and 350 K). We note that the chosen A value is consistent with those found in other liquid crystals [7.11]. Now the temperature dependence of ODF contributions came through ω_c in the cutoff function for the ODF modes. The fitting quality factor Q

is defined as

$$Q = \frac{\sum_k \sum_\omega \sum_i \sum_m \left[J_m^{(i)calc}(m\omega) - J_m^{(i)expt}(m\omega) \right]_k^2}{\sum_k \sum_\omega \sum_i \sum_m \left[J_m^{(i)expt}(m\omega) \right]_k^2} \tag{7.4}$$

where sum over i covers C_1 to C_7, sum over ω is for two different Larmor frequencies, sum over k is for fourteen temperatures covering N, SmA and N_{re} phases, and $m = 1$ and 2. We have a total of 392 spectral densities to derive ten global parameters. We found $Q = 2.8\%$ and the calculated spectral densities are shown as solid $\left(J_1^{(i)}(\omega)\right)$ and dashed $\left(J_2^{(i)}(2\omega)\right)$ curves in Figure 7.5. Although there are some systematic deviations between experimental and calculated spectral densities, the overall fits are quite satisfactory given the many simplifications (in particular the use of the "pentane" effect) in the motional model used in the present study. Figure 7.6 shows the site dependence of the experimental and calculated spectral densities at 340 K together with calculated $J_{1DF}^{(i)}(\omega)$ at the same temperature. The model parameters are summarized as plots shown in Figure 7.7. The three-bond motions are very fast and occur on the timescale of femto-second. Now k_2 increase with increasing temperature, while k_1 shows an opposite temperature behaviour. We note that the values of $D_\perp$ are very similar to those found in a dielectric study [7.12] of 8OCB, while our values of $D_\parallel$ are about an order of magnitude higher. The reason for this discrepancy is not clear. The activation energy $E_a^{D_\parallel}$ (= 49.1 kJ/mol) is higher than the activation energy $E_a^{D_\perp}$ (= 37.0 kJ/mol), which seems not physically meaningful.

This merely reflects the difficulty in getting information about the tumbling motion of the molecule, a problem often encountered in NMR studies of liquid crystals [7.13, 7.14, 7.15]. The tumbling motion ($D_\perp$) is slow with a rate less than $4 \times 10^7 s^{-1}$ just below the N-SmA transition, thereby producing some frequency dependence in both $J_1(\omega)$ and $J_2(2\omega)$ in the SmA and N_{re} phases as well as to a lesser extent in the high temperature N phase. The error limits for $E_a^{D_\parallel}$ lie between 50.1 and 47.7 KJ/mol, while 35.6 KJ/mol $< E_a^{D_\perp} <$ 38.2 KJ/mol. The error limit for a particular global parameter was estimated by varying the one under consideration while keeping all other global parameters identical to those for the minimum F, to give an approximate doubling in the F value. To examine the error limits for the jump rates, we considered k_1', k_2' and k_3' at T_{ref} ($k_1' = 1.32 \times 10^{13} s^{-1}$, $k_2' = 3.33 \times 10^{12} s^{-1}$, $k_3' = 4.1 \times 10^{16} s^{-1}$). We found that $1 \times 10^{13} s^{-1} < k_1' < 4 \times 10^{13} s^{-1}$, and $2.28 \times 10^{12} s^{-1} < k_2' < 7.5 \times 10^{12} s^{-1}$, while the lower limit of k_3' is equal to $1.58 \times 10^{15} s^{-1}$. Furthermore, any larger k_3' value does not affect the fits and hence no upper limit can be estimated. Indeed there is a tendency in the minimization to overestimate the k_3 value. The pre-exponentials in Eq. (7.2) are $D_\perp^\circ = 4.8 \times 10^{13} s^{-1}$ and $D_\parallel^\circ = 3.2 \times 10^{17} s^{-1}$. The error limits for $D_\perp^\circ$ lie between $3.1 \times 10^{13} s^{-1}$ and $7.8 \times 10^{13} s^{-1}$, while for $D_\parallel^\circ$ between $2.1 \times 10^{17} s^{-1}$ and $5.5 \times 10^{17} s^{-1}$.

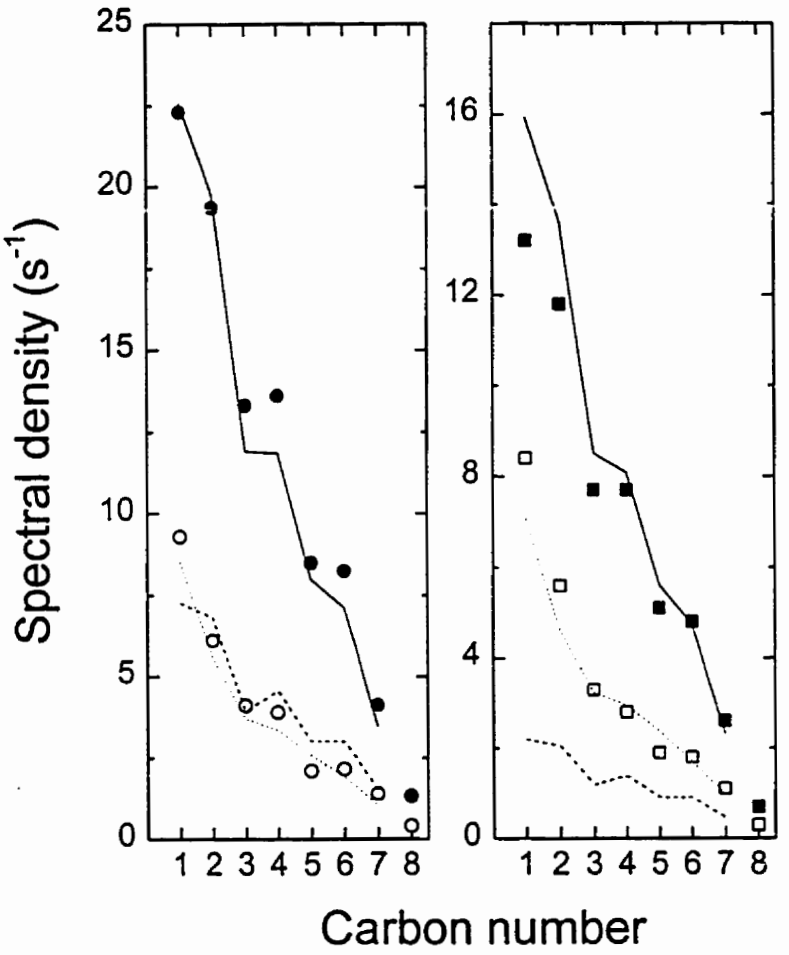

Figure 7.6 Variation of the spectral densities $J_1(\omega)$ (solid symbols) and $J_2(2\omega)$ (open symbols) with the deuteron position in the nematic phase of 8OCB/6OCB (T=340 K). Circles and squares denote data from 15.1 and 46 MHz, repectively. Solid and dotted lines are predictions for J_1 and J_2, respectively, while dashed line denotes the theoretical $J_{1DF}^{(i)}(\omega)$

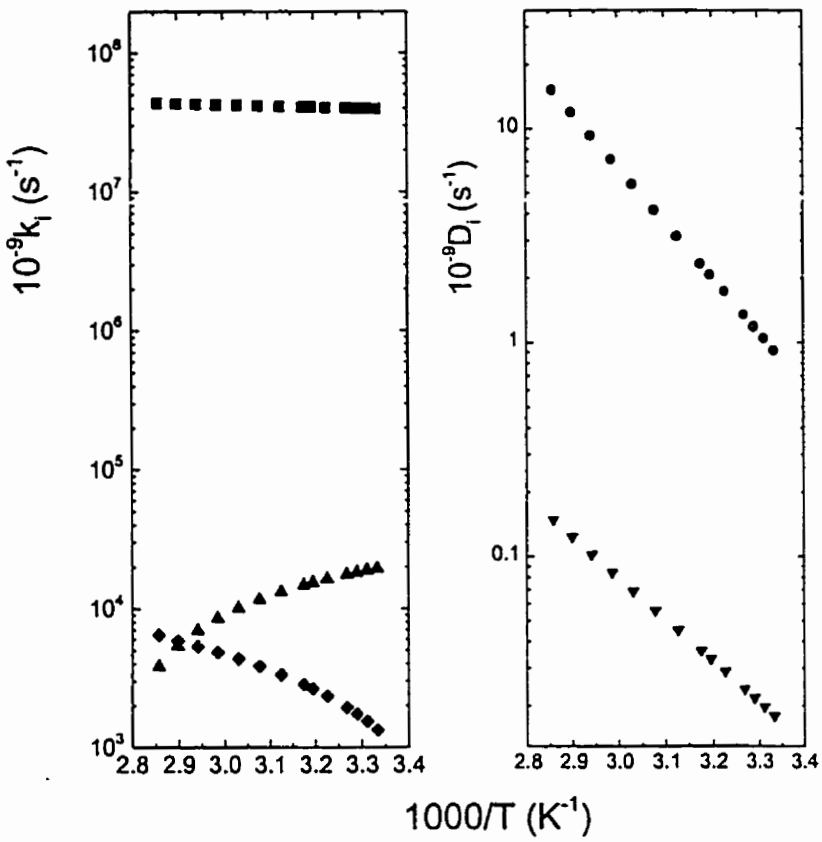

Figure 7.7 Plots of jump rate constants k_1 (uptriangle), k_2 (diamond) and k_3 (square), as well as rotational diffusion constants $D_{\parallel}$ (circle) and $D_{\perp}$ (downtriangles) as a function of the reciprocal temperature.

Strictly speaking, rotational diffusion motions of molecules in the SmA phase may well be different from that in the nematic phase, as molecules are stacked into layers. This has so far been ignored thus far as a first approximation in the literature. According

to the recent study of a biaxial probe [7.21,7.22], the effect of translation is larger on the tumbling motion than on the spinning motion, and its effect on the spectral density $J_0(\omega)$ appears to be significant at very low frequencies. It is, therefore, not clear whether the current spectral densities $J_1(\omega)$ and $J_2(2\omega)$ in the SmA phases reflect this additional refinement for molecular reorientations, especially in view of many assumptions already in place in our relaxation model. The internal dynamics of flexible chain(s) has now been studied in many different liquid crystals [7.13,7.13,7.17,7.18] using deuteron NMR and the decoupled model, and the trend towards high rates for the three-bond motion is now evident. In view of the fact that the crankshaft motion involves rather high activation energy [7.3,7.19], the relatively high k_3 values seem a bit problematic. Thus, one may have to further examine the assumptions used in the decoupled model [7.20].

References

[7.1] R. Y. Dong, Mol. Phys., **88**, 979, 1996

[7.2] R. Y. Dong, Phys. Rew. E **60**, 5631, 1999

[7.3] E. Helfand, E. R. Wasserman and T. A. Weber, Macromolecules **13**, 526, 1980

[7.4] P. Diehl and W. Niederberger, J. Magn. Reson., **15**, 391, 1974

[7.5] C. J. R. Counsell, J. W. Emsley, N. J. Heaton and G. R. Luckhurst, Mol. Phys., **54**, 847, 1985

[7.6] J. W. Emsley, G. Celebre, G. De Luca, M. Longeri, and F. Lucchesini, Liq. Cryst. **16**, 1037, 1994

[7.7] C. J. R. Counsell, PhD thesis, Southampton, 1983; C. J. R. Counsell, J. W. Emsley, G. R. Luckhurst and H. S. Sachdev, Mol. Phys., **63**, 33, 1988

[7.8] J. W. Emsley, G. R. Luckhurst, and C. P. Stockley, Proc. R. Soc. London, Ser. A, **381**, 117, 1982

[7.9] W. H. Press, B. P. Flannery, S. A. Teukolsky and W. T. Vetterling, "Numerical Pecipes", Cambridge University Press, Cambridge, England, 1986

[7.10] X. Shen and R. Y. Dong, J. Chem. Phys., **108**, 9177, 1998

[7.11] R. Y. Dong and X. Shen, J. Phys. Chem., A **101**, 4673, 1997

[7.12] S. Urban, B. Gestblom, H. Kresse and R. Dabrowski, Z. Naturforsch, **51a**, 834, 1996

[7.13] R. Y. Dong and G. M. Richards, J. Chem. Soc. Faraday Trans., **88**, 1885, 1992

[7.14] J. M. Goetz, G. L. Hoatson and R. L. Vold, J. Chem. Phys., **97**, 1306, 1992

[7.15] V. Rutar, M. Vilfan, R. Blinc and E. Bock, Mol. Phys., **35**, 721, 1978

[7.16] R. Y. Dong, Phys. Rev. A **43**, 4310, 1991

[7.17] R. Y. Dong, C. R. Morcombe, L. Calucci, M, Geppi and C. A. Veracini, Phys. Rev. E **61**, 1559, 2000

[7.18] X. Shen, R. Y. Dong, N. Boden, R. J. Bushby, P. S. Martin and A. Wood, J. Chem. Phys. **108**, 4324, 1998

[7.19] J. Skolnick and E. Helfand, J. Chem. Phys. **72**, 5489, 1980

[7.20] R. Y. Dong and M. Cheng, J. Chem. Phys., (in press)

[7.21] A. Brognara, P. Pasini, and C. Zannoni, J. Chem. Phys. **112**, 4836, 2000

[7.22] G. J. Moro and P. L. Nordio, J. Chem. Phys. **89**, 997, 1985

8 Brief Summary

Nuclear spin relaxation measurements can be used to study the molecular dynamics in liquid crystals. For MBPUB, we found an anomalous behaviour $(D_\perp > D_\parallel)$ which is different from non-chiral rodlike liquid crystals. Further NMR experiments on a chain-deuterated MBPUB and other chiral molecules of similar dimensions should be carried out to see if $D_\perp > D_\parallel$ is indeed valid at least for some chiral mesogens. When an MBPUB sample with the chiral chain deuterated is available, the additional relaxation data could be used to test a non-axial rotational diffusion tensor as described in the TZ model. Possible anomalous rotational behaviour of such chiral molecules can have significant implications on the organization and packing of tilted molecules in various chiral subphases.

For the 8OCB/6OCB mixture, a consistent picture in interpreting both the splitting and relaxation data of 8OCB in the 8OCB/6OCB mixture has emerged in the present study. In particular, the decoupled model appears to work for all three mesophases in a single global fitting method. The derived model parameters, apart from perhaps k_3 and $E_a^{D_\perp}$, are as reasonable as those found for other liquid crystals. We also found that the ODF prefactor for this system is also acceptable, and that no ODF contributions are needed for fitting the relaxation data in the reentrant nematic phase. This is simply a reflection of the viscoelastic parameters at the temperature range in which the N_{re} phase

exists in the mixture, since ODF were detected in a high temperature N_{re} phase of a pure compound [Dong, private communication]. The three-bond rotations appear to be too fast and further theoretical investigation is needed.

Appendix A Matrix Elements of the Rotational Diffusion Operator

Here we give the calculations [A.1] for the simplest and most important case for the potential of mean torque. Retain only the second rank contribution, we have

$$\frac{U(\beta,\gamma)}{kT} = a_{20}(T)\, P_2(\cos\beta) + a_{22}(T)\left[D^2_{02}(\beta,\gamma) + D^2_{0-2}(\beta,\gamma)\right] \tag{A.1}$$

where $a_{2-2} = a_{22}$ is assumed [A.2,A.3] . The ratio $\xi = a_{22}/a_{20}$, is a measure of the deviation of molecular symmetry from cylindrical symmetry. Here we separately evaluate the matrix elements of the various operators contributing to $\hat{\Gamma}$. They are

$$\begin{aligned} &\left\langle \mathcal{D}^{L'}_{mn'} \left| -\nabla^2 \right| \mathcal{D}^{L}_{mn} \right\rangle \\ &= \left[-L'(L'+1) - n'^2(\eta-1)\right] \delta_{L'L}\delta_{n'n} \,, \end{aligned} \tag{A.2}$$

$$\begin{aligned} &\left\langle \mathcal{D}^{L'}_{mn'} \left| -\frac{1}{2}\nabla^2 \frac{U(\beta,\gamma)}{kT} \right| \mathcal{D}^{L}_{mn} \right\rangle \\ &= -\frac{\sqrt{2L+1}}{2\sqrt{2L'+1}} \sum_{Jq} a_{Jq}\left[J(J+1) + (\eta-1)q^2\right] \\ &\quad \times C(L,J,L';m,0)\, C(L,J,L';n'-q,q)\, \delta_{n,n'-q} \,, \end{aligned} \tag{A.3}$$

$$\left\langle \mathcal{D}^{L'}_{mn'} \left| -\frac{1}{4}\left(L_+\frac{U(\beta,\gamma)}{kT}\right)\left(L_-\frac{U(\beta,\gamma)}{kT}\right)\right| \mathcal{D}^{L}_{mn}\right\rangle$$

$$= -\frac{\sqrt{2L+1}}{4\sqrt{2L'+1}}\sum_{Jq}\sum_{J'q'} a_{Jq}a_{J'q'}\sqrt{\left[J(J+1)-q(q+1)\right]\left[J'(J'+1)-q'(q'-1)\right]}$$

$$\times \sum_{J''=|J-J'|}^{J+J'} C(L,J'',L';0,0)\,C(L,J'',L';q+1,q'-1)\,C(L,J'',L';m,0)$$

$$\times C(L,J'',L';n'-q-q',q+q')\,\delta_{n,n'-q-q'}\ , \tag{A.4}$$

$$\left\langle \mathcal{D}^{L'}_{mn'} \left| -\frac{1}{4}\eta\left(L_z\frac{U(\beta,\gamma)}{kT}\right)\right| \mathcal{D}^{L}_{mn}\right\rangle$$

$$= -\frac{\eta\sqrt{2L+1}}{4\sqrt{2L'+1}}\sum_{Jq}\sum_{J'q'} a_{Jq}a_{J'q'}\sum_{J''=|J-J'|}^{J+J'} C(L,J',J'';0,0)\,C(L,J',J'';q,q')$$

$$\times C(L,J'',L';m,0)\,C(L,J'',L';n'-q-q',q+q')\,\delta_{n,n'-q-q'}\ , \tag{A.5}$$

$$\left\langle \mathcal{D}^{L'}_{mn'} \left| -\frac{1}{2}\epsilon\left(L_+^2+L_-^2\right)\right| \mathcal{D}^{L}_{mn}\right\rangle$$

$$= -\frac{1}{2}\epsilon\sqrt{\left[L'(L'+1)-(n'-2)(n'-1)\right]\left[L'(L'+1)-n'(n'-1)\right]}\delta_{L'L}\delta_{n,n'-2}$$

$$-\frac{1}{2}\epsilon\sqrt{\left[L'(L'+1)-(n'+2)(n'+1)\right]\left[L'(L'+1)-n'(n'+1)\right]}\delta_{L'L}\delta_{n,n'+2}\ , \tag{A.6}$$

$$\left\langle \mathcal{D}^{L'}_{mn'} \left| -\frac{1}{4}\epsilon\left(L_+^2\frac{U(\beta,\gamma)}{kT}\right)\right| \mathcal{D}^{L}_{mn}\right\rangle$$

$$= -\frac{\epsilon\sqrt{2L+1}}{4\sqrt{2L'+1}}\sum_{Jq} a_{Jq}\sqrt{\left[J(J+1)-q(q+1)\right]\left[J(J+1)-(q+1)(q+2)\right]}$$

$$\times C(L,J,L';m,0)\,C(L,J,L';n'-q-2,q+2)\,\delta_{n,n'-q-2}\ , \tag{A.7}$$

$$\left\langle \mathcal{D}^{L'}_{mn'} \left| -\frac{1}{4}\epsilon \left(L_-^2 \frac{U(\beta,\gamma)}{kT} \right) \right| \mathcal{D}^{L}_{mn} \right\rangle$$

$$= -\frac{\epsilon\sqrt{2L+1}}{4\sqrt{2L'+1}} \sum_{Jq} a_{Jq} \sqrt{[J(J+1)-q(q-1)]\,[J(J+1)-(q-1)(q-2)]}$$

$$\times C(L,J,L';m,0)\, C(L,J,L';n'-q+2,q-2)\, \delta_{n,n'-q+2}\ , \qquad \text{(A.8)}$$

$$\left\langle \mathcal{D}^{L'}_{mn'} \left| \frac{1}{8}\epsilon \left(L_+ \frac{U(\beta,\gamma)}{kT} \right)^2 \right| \mathcal{D}^{L}_{mn} \right\rangle$$

$$= \frac{\epsilon\sqrt{2L+1}}{8\sqrt{2L'+1}} \sum_{Jq} \sum_{J'q'} a_{Jq} a_{J'q'} \sqrt{[J(J+1)-q(q+1)]\,[J'(J'+1)-q'(q'+1)]}$$

$$\times \sum_{J''=|J-J'|}^{J+J'} C(L,J',J'';0,0)\, C(L,J',J'';q+1,q'+1)\, C(L,J'',L';m,0)$$

$$\times C(L,J'',L';n'-q-q'-2,q+q'+2)\, \delta_{n,n'-q-q'-2}\ , \qquad \text{(A.9)}$$

$$\left\langle \mathcal{D}^{L'}_{mn'} \left| \frac{1}{8}\epsilon \left(L_- \frac{U(\beta,\gamma)}{kT} \right)^2 \right| \mathcal{D}^{L}_{mn} \right\rangle$$

$$= \frac{\epsilon\sqrt{2L+1}}{8\sqrt{2L'+1}} \sum_{Jq} \sum_{J'q'} a_{Jq} a_{J'q'} \sqrt{[J(J+1)-q(q-1)]\,[J'(J'+1)-q'(q'-1)]}$$

$$\times \sum_{J''=|J-J'|}^{J+J'} C(L,J',J'';0,0)\, C(L,J',J'';q-1,q'-1)\, C(L,J'',L';m,0)$$

$$\times C(L,J'',L';n'-q-q'+2,q+q'-2)\, \delta_{n,n'-q-q'+2}\ . \qquad \text{(A.10)}$$

In the derivation of the matrix elements, the following relations have been used [A.4]:

$$\begin{aligned}
\nabla^2 \mathcal{D}^L_{mn} &= \left[L(L+1) + (\eta-1)n^2\right] \mathcal{D}^L_{mn} \,, \\
L_z \mathcal{D}^L_{mn} &= n \mathcal{D}^L_{mn} \,; \\
L_\pm \mathcal{D}^L_{mn} &= \sqrt{L(L+1) - n(n\pm 1)}\, \mathcal{D}^L_{m,n\pm 1} \,, \\
L^2_\pm \mathcal{D}^L_{mn} &= \sqrt{\left[L(L+1) - n(n\pm 1)\right]\left[L(L+1) - n(n\pm 1)(n\pm 2)\right]}\, \mathcal{D}^L_{m,n\pm 2} \,.
\end{aligned}$$

Now the matrix elements are

$$\begin{aligned}
\left\langle \mathcal{D}^{L'}_{mn'} \left| \hat{\Gamma} \right| \mathcal{D}^L_{mn} \right\rangle &= \left(\hat{R}^m\right)_{L'n'Ln} \\
&= \left[-L'(L'+1) - n'^2(\eta-1) + K_0\right] \delta_{L'L}\delta_{nn'} \\
&\quad -\frac{1}{2}\epsilon \sqrt{\left[L'(L'+1) - (n'-2)(n'-1)\right]\left[L'(L'+1) - n'(n'-1)\right]}\, \delta_{L'L}\delta_{n,n'-2} \\
&\quad -\frac{1}{2}\epsilon \sqrt{\left[L'(L'+1) - (n'+2)(n'+1)\right]\left[L'(L'+1) - n'(n'+1)\right]}\, \delta_{L'L}\delta_{n,n'+2} \\
&\quad +\frac{\sqrt{2L+1}}{\sqrt{2L'+1}} C(L,2,L';m,0) \left[C(L,2,L';n',0)\, K_1 \delta_{nn'}\right. \\
&\quad \left. +C(L,2,L';n'-2,2)\, K_2 \delta_{n,n'-2} + C(L,2,L';n'+2,-2)\, K_2 \delta_{n,n'+2}\right] \\
&\quad +\frac{\sqrt{2L+1}}{\sqrt{2L'+1}} C(L,4,L';m,0) \left[C(L,4,L';n',0)\, K_3 \delta_{nn'}\right. \\
&\quad \left. +C(L,4,L';n'-2,2)\, K_4 \delta_{n,n'-2} + C(L,2,L';n'+2,-2)\, K_4 \delta_{n,n'+2}\right. \\
&\quad \left. +C(L,4,L';n'-4,4)\, K_5 \delta_{n,n'-4} + C(L,4,L';n'+4,-4)\, K_5 \delta_{n,n'+4}\right] \quad \text{(A.11)}
\end{aligned}$$

where we have introduced the following auxiliary quantities:

$$
\begin{aligned}
K_0 &= -\frac{1}{5}\left(\frac{3}{2}a_{20}^2 + a_{22}^2 + \sqrt{6}\epsilon a_{20}a_{22}\right) - \frac{2}{5}\eta a_{22}^2 \\
K_1 &= -3a_{20} - \sqrt{6}\epsilon a_{22} - \frac{1}{7}\left(\frac{3}{2}a_{20}^2 + a_{22}^2 + \sqrt{6}\epsilon a_{20}a_{22}\right) + \frac{4}{7}\eta a_{22}^2 \\
K_2 &= -(1+2\eta)\, a_{22} - \frac{\sqrt{6}}{2}\epsilon a_{20} + \frac{\sqrt{6}}{7}\left(\frac{\sqrt{6}}{2}a_{20}a_{22} + \frac{3}{4}\epsilon a_{20}^2 + \frac{1}{2}\epsilon a_{22}^2\right) \\
K_3 &= \frac{12}{35}\left(\frac{3}{2}a_{20}^2 + a_{22}^2 + \sqrt{6}\epsilon a_{20}a_{22}\right) - \frac{6}{35}\eta a_{22}^2 \\
K_4 &= \frac{6}{7}\sqrt{\frac{2}{5}}\left(\frac{\sqrt{6}}{2}a_{20}a_{22} + \frac{3}{4}\epsilon a_{20}^2 + \frac{1}{2}\epsilon a_{22}^2\right) \\
K_5 &= 3\sqrt{\frac{2}{35}}\eta a_{22}^2
\end{aligned}
\tag{A.12}
$$

Here the symmetry relation $C(2,2,J;m,n) = (-1)^J C(2,2,J;-m,-n)$ has been used. We have also substituted explicit values [A.5] for the Clebsch-Gordon coefficients, where possible.

References

[A.1] R. Tarroni and C. Zannoni, J. Chem. Phys., 95, 4550, 1991

[A.2] G. R. Luckhurst, "The Molecular Physics of Liquid Crystals", edited by G. R. Luckhurst and G. W. Gray, Academic, New York, 1979

[A.3] F. Biscarini, C. Chiccoli, P. Pasini, F. Semeria and C. Zannoni, 14th International Liquid Crystal Conference, 1992

[A.4] M. E. Rose, "Elementary Theory of Angular Momentum", Wiley, New York, 1957

[A.5] P. Pasini and Z. Zannoni, "INFN Bull", TC-83/19, 1, 1984